

การสังเคราะห์ซิลิคอนไนไตรด์พูนด้วยกระบวนการคาร์โบเทอร์มอลรีดักชันและไนไตรเดชัน

ของชิลิกา/ฟิอาร์เอฟเจล คอมพอสิต

นางสาวมาริษา มีชูนิก

วิทยานิพนธ์นี้เป็นส่วนหนึ่งของการศึกษาตามหลักสูตรปริญญาวิศวกรรมศาสตรมหาบัณฑิต

สาขาวิชาวิศวกรรมเคมี ภาควิชาวิศวกรรมเคมี

คณะวิศวกรรมศาสตร์ จุฬาลงกรณ์มหาวิทยาลัย

ปีการศึกษา 2554

ลิขสิทธิ์ของจุฬาลงกรณ์มหาวิทยาลัย

บทคัดย่อและแฟ้มข้อมูลฉบับเต็มของวิทยานิพนธ์ตั้งแต่ปีการศึกษา 2554 ที่ให้บริการในคลังปัญญาจุฬาฯ (CUIR)
เป็นแฟ้มข้อมูลของนิสิตเจ้าของวิทยานิพนธ์ที่ส่งผ่านทางบัณฑิตวิทยาลัย

The abstract and full text of theses from the academic year 2011 in Chulalongkorn University Intellectual Repository(CUIR)
are the thesis authors' files submitted through the Graduate School.

SYNTHESIS OF POROUS SILICON NITRIDE VIA
THE CARBOTHERMAL REDUCTION AND NITRIDATION OF
SILICA/PRF GEL COMPOSITE

Miss Marisa Meechoonuck

A Thesis Submitted in Partial Fulfillment of the Requirements for the
Degree of Master of Engineering Program in Chemical Engineering

Department of Chemical Engineering

Faculty of Engineering

Chulalongkorn University

Academic Year 2011

Copyright of Chulalongkorn University

Thesis Title SYNTHESIS OF POROUS SILICON NITRIDE VIA
 THE CARBOTHERMAL REDUCTION AND
 NITRIDATION OF SILICA/PRF GEL COMPOSITE
By Miss Marisa Meechoonuck
Field of Study Chemical Engineering
Thesis Advisor Assistant Professor Varong Pavarajarn, Ph.D.

Accepted by the Faculty of Engineering, Chulalongkorn University in
Partial Fulfillment of the Requirements for the Master's Degree

..... Dean of the Faculty of Engineering
(Associate Professor Boonsom Lerdhirunwong, Dr.Ing.)

THESIS COMMITTEE

..... Chairman
(Associate Professor Sarawut Rimdusit, Ph.D.)

..... Thesis Advisor
(Assistant Professor Varong Pavarajarn, Ph.D.)

..... Examiner
(Associate Professor Tawatchai Charinpanitkul, D.Eng.)

..... External Examiner
(Chanchana Thanachayanont, Ph.D.)

มาริษา มีชุนี : การสังเคราะห์ซิลิคอนไนไตรด์พูนด้วยกระบวนการคาร์โบเทอร์มอลรีดักชันและไนไตรเดชันของซิลิกา/พอร์เอฟเจล คอมพอสิต (SYNTHESIS OF POROUS SILICON NITRIDE VIA THE CARBOTHERMAL REDUCTION AND NITRIDATION OF SILICA/PRF GEL COMPOSITE) อ. ที่ปรึกษาวิทยานิพนธ์หลัก:
 ผศ.ดร.วรงค์ ปวรจารย์, 81 หน้า.

งานวิจัยนี้ศึกษาการสังเคราะห์ซิลิคอนไนไตรด์พูนซึ่งเป็นวัสดุที่มีโครงสร้างเหมาะสมสำหรับใช้งานในการกรองภายใต้อุณหภูมิสูงจากซิลิกา/ฟีนอล-เรโซซินอล-ฟอร์มัลดีไฮด์(พอร์เอฟ)เจลคอมพอสิตที่ถูกเตรียมด้วยวิธีโซล-เจลร่วมกับปฏิกิริยาโพลีเมอไรเซชันของฟีนอล, เรโซซินอล และฟอร์มัลดีไฮด์โดยใช้โซเดียมคาร์บอเนตเป็นตัวเร่งปฏิกิริยา และใช้ 3-อะมิโนโพรพิล ไตรเมทอกซีไซเลน (เอพีทีเอ็มเอส) เป็นสารตั้งต้นของซิลิกา หลังจากนั้นสารผสมจะถูกอบไว้ที่ 72 ชั่วโมงก่อนที่จะมีการแลกเปลี่ยนตัวทำละลายในสารผสมด้วย ที-บิวทานอล ทุก 24 ชั่วโมง เป็นเวลา 3 วัน ก่อนที่จะนำไปอบแห้งแบบเยือกแข็งที่อุณหภูมิ -40 องศาเซลเซียส เป็นเวลา 3 วัน จากนั้น นำซิลิกา/พอร์เอฟคอมพอสิตไปผ่านกระบวนการไพโรไลซิส ภายใต้แก๊สไนโตรเจนและกระบวนการแคลซิเนชันรอบแรกภายใต้อากาศที่อุณหภูมิ 400-500 องศาเซลเซียสเป็นเวลา 2 ชั่วโมงเพื่อกำจัดโครงสร้างพอร์เอฟและคาร์บอนบางส่วนออกให้กลายเป็นซิลิกา/คาร์บอนคอมโพสิตพูน สุดท้ายจะนำคอมโพสิตที่ได้เข้าสู่กระบวนการไนไตรเดชันที่อุณหภูมิ 1450 องศาเซลเซียสเป็นเวลา 10 ชั่วโมง แล้วเผาทำจัดการ์บอนส่วนที่เหลือออกอีกครั้งที่อุณหภูมิ 800 องศาเซลเซียสเป็นเวลา 8 ชั่วโมง จากการทดลองพบว่า อัตราส่วนโมลของฟีนอล, เรโซซินอล, ซิลิกา, คาร์บอนและอุณหภูมิที่ใช้ในการแคลซิเนชันเพื่อกำจัดการ์บอนบางส่วนออกที่แตกต่างกัน ส่งผลต่อความพรุนของซิลิกา/คาร์บอน คอมโพสิตและซิลิคอนไนไตรด์ที่แตกต่างกันด้วย โดยการปรับแคลซิเนชันที่เป็นตัวแปรหลักทำให้เกิดการปรับปรุงความพรุนของคอมโพสิต ซึ่งส่งผลต่อความพรุนของซิลิคอนไนไตรด์ นอกจากนี้ยังพบว่า การเตรียมสารตั้งต้นซิลิกาให้อยู่ในรูปของโซลก่อนเติมลงไปไนพอร์เอฟเจลก็เป็นอีกทางเลือกหนึ่งในการลดความรุนแรงของปฏิกิริยาระหว่างซิลิกาและสารละลายพอร์เอฟ ก็ส่งผลต่อความพรุนและขนาดผลึกของซิลิคอนไนไตรด์

ภาควิชา.....วิศวกรรมเคมี.....ลายมือชื่อนิสิต.....

สาขาวิชา.....วิศวกรรมเคมี.....ลายมือชื่อ อ.ที่ปรึกษาวิทยานิพนธ์หลัก.....

ปีการศึกษา.....2554.....

5370475621: MAJOR CHEMICAL ENGINEERING

KEYWORDS: SILICON NITRIDE / POROUS / CARBOTHERMAL
REDUCTION AND NITRIDATION / PHENOL / RESORCINOL /
FORMALDEHYDE GEL

MARISA MEECHOONUCK: SYNTHESIS OF POROUS SILICON NITRIDE
VIA THE CARBOTHERMAL REDUCTION AND NITRIDATION OF
SILICA/PRF GEL COMPOSITE

ADVISOR: ASST. PROF. VARONG PAVARAJARN, Ph.D., 81 pp.

This research studied the synthesis of porous silicon nitride, one of the most promising structural materials for applications in filter at high-temperature, from silica/phenol-resorcinol-formaldehyde (PRF) gel composite which was prepared by combining sol-gel and polymerization of phenol, resorcinol and formaldehyde using sodium carbonate as catalyst and 3-aminopropyl trimethoxysilane (APTMS) as silica precursor. After aging of the silica/PRF gel for 72 hours, *t*-butanol was used in the solvent exchange process for 24 hours and repeated for 3 times. Then the sample was dried in freeze drying processes at -40°C for 3 days. Next, the silica/PRF composite was pyrolyzed under nitrogen gas and pre-calcined first under air at temperature in the range of $400\text{-}500^{\circ}\text{C}$ for 2 hours to convert the PRF structure into porous carbon and partially remove carbon from the composite, respectively. Finally, the composite was subjected to the carbothermal reduction and nitridation at 1450°C for 10 hours followed by the removal of residual carbon by calcination at 800°C for 8 hours. From the results, differences in molar ratio of phenol-to-resorcinol, silica-to-carbon and pre-calcination temperature result in difference in porosity of both silica/carbon composite and that of silicon nitride product. The pre-calcination is the major effect to improve the porosity, which has an effect on porosity of silicon nitride product. Moreover, it was also found that the use of pre-formed silica sol, which is another way to decrease violent interaction between silica precursor and the PRF solution, has an effect on porosity and crystallite size of silicon nitride product.

Department: ...Chemical Engineering...Student's Signature:

Field of Study: ..Chemical Engineering...Advisor's Signature:

Academic Year: ...2011...

ACKNOWLEDGEMENTS

The authors want to dedicate all of this research to the person that relate to my successful. Assistant Professor Dr. Varong Pavarajarn, for his friendly, kindness, valuable suggestions, useful discussions throughout this research and devotion to revise this thesis; otherwise, this research work could not be completed. In addition, the author would also be grateful to Associate Professor Dr. Sarawut Rimdusit, as the chairman, Associate Professor Dr. Tawatchai Charinpanitkul, and Dr. Chanchana Thanachayanont, as the members of the thesis committee.

Most of all, the author would like to express my highest gratitude to my parents who always pay attention to me all the times for suggestions and their wills. The most success of graduation is devoted to my parents.

Finally, the author wishes to thank the member of the Center of Excellence in Particle technology, Department of Chemical Engineering, Faculty of Engineering, Chulalongkorn University for their assistance.

CONTENTS

	Page
ABSTRACT (THAI).....	iv
ABSTRACT (ENGLISH).....	v
ACKNOWLEDGEMENTS.....	vi
CONTENTS.....	vii
LIST OF TABLES.....	ix
LIST OF FIGURES.....	xii
CHAPTER	
I INTRODUCTION.....	1
II THEORY AND LITERATURE SURVEY.....	4
2.1 Silicon nitride.....	4
2.1.1 Crystal structure of silicon nitride.....	5
2.1.2 Properties of silicon nitride ceramic.....	7
2.2 Carbothermal reduction and nitridation of silica.....	9
2.3 Sol-Gel processing.....	10
2.4 Resorcinol–formaldehyde (RF) gel.....	12
2.5 Phenol–formaldehyde (PF) gel.....	15
III EXPERIMENTAL.....	19
3.1 Chemicals.....	19
3.2 Preparation of silica/PRF gel.....	19
3.3 Preparation of porous silica/carbon composite.....	20
3.4 Carbothermal reduction and nitridation of silica/carbon composite.....	21
3.5 Characterizations of the products.....	22
3.5.1 X-ray diffraction analysis (XRD).....	22

	Page
3.5.2	Fourier-transform infrared spectroscopy (FT-IR)22
3.5.3	Scanning electron microscopy (SEM).....22
3.5.4	Transmission electron microscopy (TEM)23
3.5.5	Surface area measurement23
3.5.6	Thermogravimetric analysis (TGA)23
IV	RESULTS AND DISCUSSION24
4.1	Effect of phenol-to-resorcinol molar ratio.....30
4.2	Effect of silica-to-carbon molar ratio41
4.3	Effect of the calcination of the pyrolyzed composite48
4.4	The use of silica sol as silica source53
V	CONCLUSIONS AND RECOMMENDATIONS59
5.1	Summary of the results59
5.2	Conclusions60
5.3	Recommendations for future work60
	REFERENCES62
	APPENDICES67
APPENDIX A	CALCULATION OF MOLAR RATIO OF SILICA AND CARBON IN PRF GEL COMPOSITE.....68
APPENDIX B	DATA OF SURFACE AREA AND AVG. PORE DIAMETER.....70
APPENDIX C	CALIBRATION CURVES FOR GAS FLOW METER OF SYNTHESIS GAS.....76
APPENDIX D	CALCULATION OF THE CRYSTALLITE SIZE77
APPENDIX E	LIST OF PUBLICATION.....77
VITA81

LIST OF TABLES

Table	Page
2.1 Typical properties of silicon nitride powders produced by various processing techniques	5
2.2 Properties of silicon nitride ceramics.....	7
4.1 Assignments of FTIR absorption bands of the dried silica/PRFgels	31
4.2 Specific surface area and carbon content of pyrolyzed silica/PRF composites after being calcined at 500°C for 2 h. The composites were prepared by pyrolysis of silica/PRF gels synthesized with various molar ratios of P-to-R, compared with that of pyrolyzed silica/PF gel, and pyrolyzed silica/RF gel	35
4.3 TGA analysis of the samples after being freeze-dried (silica/PRF gel) and after being pyrolyzed (i.e., silica/carbon composites), prepared using various P-to-R molar ratios. The SiO ₂ /C molar ratio was fixed at 0.05	37
4.4 Crystallite sizes of silicon nitride powder, after the final calcination at 800°C for 8 h. The products were synthesized from silica/PRF composites with various molar ratios of P-to-R	39
4.5 Surface area and % mass loss from TGA analysis in oxygen atmosphere of silicon nitride products after final calcination. The composites were prepared from SiO ₂ /PRF gel with various molar ratios of P-to-R, which was pre-calcined at 500°C for 2 h.....	40
4.6 Crystallite sizes of silicon nitride powder, after the final calcination at 800°C for 8 h. The products were synthesized from silica/PRF composites with various molar ratios of SiO ₂ /C.....	43
4.7 Surface areas of pyrolyzed silica/carbon composite and final products silicon nitride synthesized with various SiO ₂ /C molar ratios	45
4.8 Mass loss from TGA analysis of silicon nitride products after the final calcination. The analysis were done in oxygen atmosphere. The composites were prepared from silica/PRF gel with various molar ratios of SiO ₂ /C.....	45

4.9 Specific surface area and carbon content of silica/carbon composite after being calcined and that of the final nitrated product, as a function of the calcination temperature of the silica/carbon composite.....	49
4.10 Crystallite sizes of silicon nitride powder, after calcination at 800°C for 8 h. The products were prepared from silica/PRF composite with P/R and Si/C ratio 0.3 and 0.03. The silica/carbon composites were calcined at various calcination temperatures: (a) 400°C, (b) 450°C and (c) 500°C before nitridation.....	53
4.11 Crystallite sizes of silicon nitride powder, after calcination at 800°C for 8 h. The products were prepared from synthesized using APTMS and pre-formed silica sol as the silica source. The P/R and SiO ₂ /C molar ratio were fixed at 0.3 and 0.03, respectively	54
4.12 Specific surface areas and carbon content of pyrolyzed silica/carbon composite and the final nitride products after calcination at 800°C for 8 h. The products were prepared from synthesized using APTMS and pre-formed silica sol as the silica source. The P/R and SiO ₂ /C molar ratio were fixed at 0.3 and 0.03, respectively	56
B.1 Data of surface area and average pore diameter of pyrolyzed silica/PRF composites after being calcined at 400°C for 2 h	70
B.2 Data of surface area and average pore diameter of pyrolyzed silica/PRF composites after being calcined at 450°C for 2 h	71
B.3 Data of surface area and average pore diameter of pyrolyzed silica/PRF composites after being calcined at 500°C for 2 h	72
B.4 Data of surface area and average pore diameter of silicon nitride product after final calcination at 800°C for 8 h. The pyrolyzed silica/PRF composites were calcined at 400°C for 2 h.....	73
B.5 Data of surface area and average pore diameter of silicon nitride product after final calcination at 800°C for 8 h. The pyrolyzed silica/PRF composites were calcined at 450°C for 2 h.....	74

Page

B.6 Data of surface area and average pore diameter of silicon nitride product after final calcination at 800°C for 8 h. The pyrolyzed silica/PRF composites were calcine at 500°C for 2 h.....	75
------------------------------------------------------------------------------------------------------------------------------------------------------------------------------------------------	----

LIST OF FIGURES

Figure	Page
2.1 α - Si_3N_4 unit cell: the structure of α - Si_3N_4 can be described as a stacking of Si-N layers in ...ABCDABCD... sequence.....	6
2.2 β - Si_3N_4 unit cell: the structure of β - Si_3N_4 can be described as a stacking of Si-N layers in ...ABAB... sequence.....	6
2.3 Crystal structure of γ - Si_3N_4	7
2.4 Sol-gel process and their products	11
2.5 Molecular presentation of the polymerization mechanism of resorcinol with formaldehyde	13
2.6 Gel formation in the resorcinol-formaldehyde system	14
2.7 A schematic diagram of the reaction of phenol and formaldehyde catalyzed by alkaline catalyst	16
3.1 Schematic diagram of the tubular flow reactor used for the preparation of silica/carbon composite	20
3.2 Schematic diagram of the tubular flow reactor used for the carbothermal reduction and nitridation.....	21
4.1 SEM micrographs of silica PRF composite prepared by using P/R molar ratio of 0.5 and the SiO_2/C molar ratio of 0.05: (a) after pyrolysis (b) after pyrolysis and first calcination, (c) after nitridation and (d) after final calcination.....	25
4.2 TEM micrographs and SAED patterns of silica/PRF composite prepared by using P/R molar ratio of 0.5 and the SiO_2/C molar ratio of 0.05: (a) before pyrolysis and (b) after being pyrolysis and first calcination.....	27
4.3 TEM micrographs and SAED pattern of silica/PRF composite prepared by using P/R molar ratio of 0.5 and the SiO_2/C molar ratio of 0.05: (a) after nitridation and (b) after final calcination.....	28

4.4 XRD patterns of silicon nitride product, after calcination at 800°C for 8 h. The products were synthesized with P/R molar ratio of 0.5 and SiO ₂ /C molar ratio of 0.05	29
4.5 FTIR spectrum of dried silica/PRF gel prepared by using P/R molar ratio of 0.3 (a), 0.5 (b), 1.0 (c), 1.5 (d), compared with that of silica/PF gel (e), and silica/RF gel (f)	31
4.6 SEM micrographs of pyrolyzed silica/PRF composites. The composites were prepared by pyrolysis of silica/PRF gels using P/R molar ratio of 0.3 (a), 0.5 (b), 1.0 (c), 1.5 (d), compared with that of pyrolyzed silica/PF composite (e), and pyrolyzed silica/RF composite (f)	33
4.7 Pore size distribution of pyrolyzed silica/PRF composites after being calcined at 500°C for 2 h. The composites were prepared by pyrolysis of silica/PRF gels synthesized with various molar ratios of P-to-R	36
4.8 XRD patterns of silicon nitride powder, after the final calcination at 800°C for 8 h. The products were synthesized with P/R molar ratios of 0.3 (a), 0.5 (b), 1.0 (c), 1.5 (d), compared with that synthesized from silica/PF composite (e), and silica/RF composite (f). The SiO ₂ /C molar ratio was fixed at 0.05	38
4.9 FTIR spectrum of silica/carbon composite prepared by using P/R molar ratio of 0.3 and various SiO ₂ /C molar ratios of 0.03 (a), 0.05 (b) and 0.07 (c)	41
4.10 XRD patterns of silicon nitride powder, after the final calcination at 800°C for 8 h. The products were synthesized with SiO ₂ /C molar ratios of 0.03 (a), 0.05 (b), and 0.07 (c). The P/R molar ratio was fixed at 0.3	42
4.11 SEM micrographs of the silicon nitride products synthesized with various SiO ₂ /C molar ratios, after the final calcination: (a) 0.03; (b) 0.05 and (c) 0.07	44

4.12 Pore size distribution of pyrolyzed silica/PRF composites after being calcined at 450°C for 2 h. The samples were prepared by pyrolysis of silica/PRF gels synthesized with various molar ratios of SiO ₂ /C	46
4.13 Pore size distribution of silicon nitride product, after the final calcination at 800°C for 8 h. The products were prepared by pyrolysis of silica/PRF gels synthesized with various molar ratios of SiO ₂ /C	47
4.14 Adsorption and desorption isotherms of N ₂ on silicon nitride products, after the final calcination at 800°C for 8 h. The products were prepared by pyrolysis of silica/PRF gels synthesized with various molar ratios of SiO ₂ /C	48
4.15 Pore size distributions of the silica/carbon composites after the 1 st calcination at various temperatures. The samples were prepared from silica/PRF composite synthesized with P/R and SiO ₂ /C ratio of 0.3 and 0.03, respectively.....	50
4.16 Pore size distributions of the final products after the 2 nd calcination. The samples were prepared from silica/PRF composite synthesized with P/R and SiO ₂ /C ratio of 0.3 and 0.03, respectively and subjected to the 1 st calcination at various temperatures	51
4.17 XRD patterns of silicon nitride powder, after the final calcination at 800°C for 8 h. The products were prepared from silica/PRF composite with P/R and SiO ₂ /C ratio 0.3 and 0.03. The silica/carbon composites were calcined at various calcination temperatures: (a) 400°C, (b) 450°C and (c) 500°C before nitridation	52

4.18	XRD patterns of silicon nitride powder, after the final calcination at 800°C for 8 h. The products were prepared from synthesized using APTMS (a) and pre-formed silica sol (b) as the silica source. The P/R and SiO ₂ /C molar ratio were fixed at 0.3 and 0.03, respectively	54
4.19	SEM micrographs of the silicon nitride products after final calcination. The products were prepared from synthesized using APTMS and pre-formed silica sol as the silica source. The P/R and SiO ₂ /C molar ratio were fixed at 0.3 and 0.03, respectively	55
4.20	Pore size distributions of the silica/carbon composites after 1 st calcination. The composites were prepared from synthesized using APTMS and pre-formed silica sol as the silica source. The P/R and SiO ₂ /C molar ratio were fixed at 0.3 and 0.03, respectively	57
4.21	Pore size distributions of the silicon nitride products after final calcination. The products were prepared from synthesized using APTMS and pre-formed silica sol as the silica source. The P/R and SiO ₂ /C molar ratio were fixed at 0.3 and 0.03, respectively	57
4.22	Adsorption and desorption isotherms of N ₂ on silicon nitride products, after calcination at 800°C for 8 h. The products were prepared from synthesized using APTMS and pre-formed silica sol as the silica source. The P/R and SiO ₂ /C molar ratio were fixed at 0.3 and 0.03, respectively	58
C.1	The calibration curve of argon	76
C.2	The calibration curve of nitrogen	76
D.1	The plot indicating the value of line broadening due to the equipment. The data were obtained by using quartz as standard	79

CHAPTER I

INTRODUCTION

Silicon nitride (Si_3N_4) is one of the most promising advanced ceramic materials. It has been extensively studied for high temperature applications because of unique properties such as low density, high-temperature strength, high stress and damage tolerance, excellent thermal shock resistance, and high reliability comparing to most ceramics. In the common applications of silicon nitride, it has been used as structural components of gas turbines, reciprocating engine parts, membranes, catalyst supports, cutting tools, bearings, and metal forming components [1].

Silicon nitride exists in two major hexagonal crystallographic forms, i.e., α -phase and β -phase [2]. β - Si_3N_4 is more desirable structure for high-temperature engineering applications because of its high-temperature strength and excellent thermal shock resistance. Fabrication of β - Si_3N_4 parts usually starts from α - Si_3N_4 powder mixed with sintering additives which is subsequently sintered at high temperature. During the sintering process, transformation from α -phase to β -phase occurs, providing desirable microstructure having high mechanical and thermal strength [3].

Si_3N_4 powders can be produced by the several methods such as direct nitridation of silicon, carbothermal reduction and nitridation of silica, diimide synthesis, and vapor phase synthesis. Nevertheless, one of the most popular methods for Si_3N_4 synthesis is the carbothermal reduction and nitridation of silica. This process involves reaction of carbon and silica in nitrogen atmosphere at temperature in the range from 1200°C to 1450°C [4].

Porous ceramics are essential for many industries, where high surface area and insulating characteristics are required. Porosity in ceramic reduces density of specimen. With the expansion of applications for porous ceramics, high porosity as well as high strength is required at the same time. Porous ceramics have also been attracting great interest for various applications relating to separation in severe environments, in which other materials such as metals or organic materials can not be used.

Porous silicon nitride has attracted great interest for engineering applications. Its high strength at high temperature, good thermal stress resistance due to the low coefficient of thermal expansion, and relatively good resistance to oxidation comparing to other high-temperature materials make porous silicon nitride to be a very good candidate for applications such as high-temperature gas filter and catalyst carriers.

Many researchers have studied the preparation of porous silicon nitride and silicon nitride-based composites. Properties of the porous silicon nitride ceramics are influenced by their relative density and morphology of grains and pores (e.g., grain size, aspect ratio, pore size and amount) [5]. The porous silicon nitride ceramics can be fabricated by using the fugitive substance [6], partial sintering [7], restrained sintering [8,9], partial hot-pressing [10], and freeze-drying [11].

In this work, resorcinol-formaldehyde (RF) gel was used as a carbon source for the carbothermal reduction with silica. It was prepared from resorcinol and formaldehyde according to the method proposed by Pekala [12]. The RF gel can be converted into highly porous carbon gel via the pyrolysis. When phenol is used in place of resorcinol, the phenol-formaldehyde (PF) gel, which can also be pyrolyzed into porous carbon aerogel as well, is obtained. Although the structures of RF and PF gel are similar, the oxidation of carbon derived from RF and PF gels was found to occur at different temperature [13].

In this research, both phenol and resorcinol was used to form phenol-resorcinol-formaldehyde (PRF) gel. Silica was incorporated into the PRF gel via the sol-gel process. The silica/carbon composite formed by the pyrolysis of the dried silica/PRF gel was used as a precursor for the carbothermal reduction and nitridation to produce silicon nitride, of which the porosity was controlled by porous structure of the silica/PRF gel. This work focuses on effects of various factors, such as composition of the PRF-gel, silica-to-carbon molar ratio of the composites, controlled calcination temperature to partially remove carbon from the silica/carbon composite to enhance porosity of the composite, and the alteration of the silica precursor into preformed silica sol.

This thesis is divided into five chapters. The first three chapters describe general information about the study, while the following two chapters emphasize on the results and discussion from the present study. Chapter I is the introduction of this work. Chapter II describes basic theory about silicon nitride properties, the carbothermal reduction and nitridation process, sol-gel process, resorcinol-formaldehyde (RF) gel, and phenol-formaldehyde (PF) gel. Chapter III shows materials and experimental systems. Chapter IV presents the experimental results and discussion. In the last chapter, the overall conclusions from the results and recommendation for future work are presented.

CHAPTER II

THEORY AND LITERATURE SURVEY

2.1 Silicon nitride

Silicon nitride (Si_3N_4) has been regarded as one of the most promising advanced ceramic materials which have to be synthesized because it does not exist in nature. It is not easy to obtain the silicon nitride powders with high purity, fine grain size and narrow size distribution. These characteristics are significant for the fabrication of silicon nitride specimen [14].

The following techniques are usually applied to synthesize Si_3N_4 powders [4] : (1) direct nitridation of metallic silicon powder, (2) gas-phase reaction of SiCl_4 , (3) carbothermal reduction and nitridation of SiO_2 in nitrogen atmosphere, and (4) precipitation and thermal decomposition of silicon diimide. For the industrial production of silicon nitride powders, silica, silicon, and silicon tetrachloride (SiCl_4) are the three commonly used starting materials for the mentioned processes, owing to their high purity. They can also be easily purified. Properties of the powders produced via these techniques may be changed by varying the processing conditions as shown in Table 2.1 [15].

Table 2.1 Typical properties of silicon nitride powders produced by various processing techniques [15].

Properties	Direct nitridation of silicon	Vapor phase synthesis	Carbothermal nitridation	Diimide synthesis
Specific surface area (m ² /g)	8-25	3.7	4.8	10
Oxygen content (wt %)	1.0-2.0	1	1.6	1.4
Carbon content (wt %)	0.1-0.4	-	0.9-1.1	0.1
Metallic impurities (wt %)	0.07-0.15	0.03	0.06	0.005
Crystallinity (%)	100	60	100	100
$\alpha/(\alpha+\beta)$ (%)	95	95	95	85

2.1.1 Crystal structure of silicon nitride

Silicon nitride exists in three crystallographic forms. The structures are designated as α , β , and γ -phase. While the α and β phases can be produced under normal nitrogen pressure and have a great importance in the production of advanced ceramics, the recently discovered γ -Si₃N₄ can be formed only at extremely high pressure [16] and has no practical use yet.

In the process of manufacturing silicon nitride specimen, the α -phase is generally preferred as basic raw material because of the desirable microstructural characteristics obtained during the phase transformation into β -phase at high temperature. Detailed X-ray diffractometry (XRD) examinations in the mid-1950s

have proved that the crystal structure of both α and β polymorphs are hexagonal [2]. However, their respective structural dimensions are different. The structures of α , β and γ -phase are shown in Figure 2.1, 2.2 and 2.3 respectively.

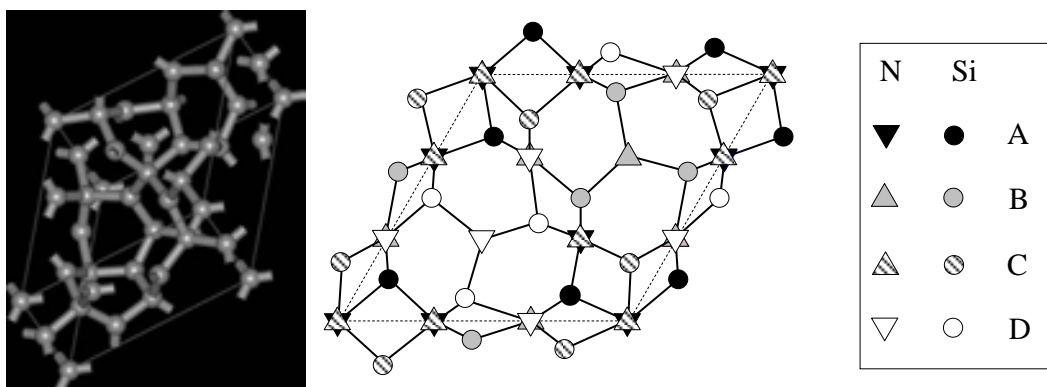


Figure 2.1 α - Si_3N_4 unit cell: the structure of α - Si_3N_4 can be described as a stacking of Si-N layers in ...ABCDABCD... sequence.

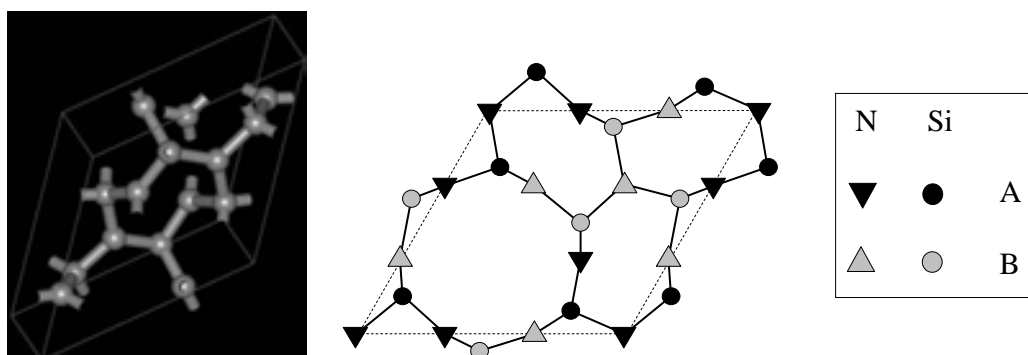


Figure 2.2 β - Si_3N_4 unit cell: the structure of β - Si_3N_4 can be described as a stacking of Si-N layers in ...ABAB... sequence.

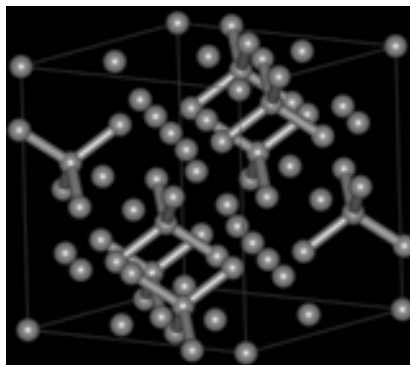


Figure 2.3 Crystal structure of γ - Si_3N_4

2.1.2 Properties of silicon nitride ceramic

The properties of silicon nitride ceramics depend on two types of silicon nitride, i.e., dense Si_3N_4 and porous Si_3N_4 . The former can be produced by pressureless sintering, hot-pressing or hot-isostatic pressing, all of which were controlled by a liquid-phase sintering. The latter can be produced by using the fugitive substance [6], partial sintering [7], restrained sintering [8,9], partial hot-pressing [10], freeze-drying [11], and reaction-bonding of silicon powder compacts [17]. The properties of two types of silicon nitride specimens are shown in Table 2.2 [4]

Table 2.2 Properties of silicon nitride ceramics.

Theoretical density (g cm^{-3}):	
α -phase	3.168-3.188
β -phase	3.19-3.202
Density (g cm^{-3}):	
dense Si_3N_4	90-100% th.d.*
reaction-bonded Si_3N_4	70-88% th.d.
Coefficient of thermal expansion (20-1500°C) (10^{-6}C^{-1})	2.9-3.6

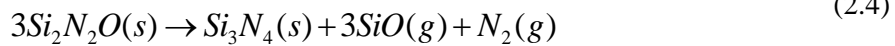
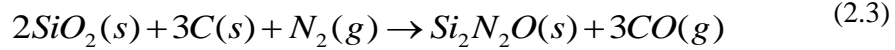
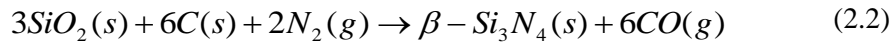
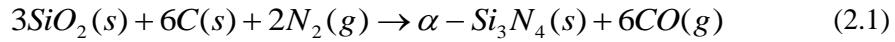
Table 2.2 (Continued).

Thermal conductivity (RT) ($\text{W m}^{-1}\text{K}^{-1}$): dense Si_3N_4 reaction-bonded Si_3N_4	15-50 4-30
Thermal diffusivity (RT) ($\text{cm}^2 \text{sec}^{-1}$): dense Si_3N_4 reaction-bonded Si_3N_4	0.08-0.29 0.02-0.22
Specific heat ($\text{J kg}^{-1} \text{°C}^{-1}$)	700
Electrical resistivity (RT) ($\Omega \text{ cm}$)	$\sim 10^{13}$
Microhardness (Vickers, MN m^{-2})	1600-2200
Young's modulus, (RT) (GN m^{-2}): dense Si_3N_4 reaction-bonded Si_3N_4	300-330 120-220
Flexural strength (RT) (MN m^{-2}): dense Si_3N_4 reaction-bonded Si_3N_4	400-95 150-350
Fracture toughness ($\text{MN m}^{-3/2}$): dense Si_3N_4 reaction-bonded Si_3N_4	3.4-8.2 1.5-2.8
Thermal stress resistance parameter $R = \sigma_F(1-\nu)/\alpha E$ (°C) and $R' = R\lambda$ (10^3 W m^{-1}): dense Si_3N_4 reaction-bonded Si_3N_4	$R = 300-780$ $R' = 7-32$ $R = 220-580$ $R' = 0.5-10$

th.d.* = Theoretical density is dependent on the type and composition of consolidation aids (Theoretical density of pure $\text{Si}_3\text{N}_4 = 3.2 \text{ g cm}^{-3}$)

2.2 Carbothermal reduction and nitridation of silica

The carbothermal reduction and nitridation of silica powder under nitrogen is the earliest method to synthesize silicon nitride and silicon carbide. This technique also showed the possibility of synthesizing highly porous and strong silicon nitride materials at considerably lower cost than at present. The reaction starts from a mixture of silica and carbon, of which the reaction with nitrogen at high temperature in the range from 1400°C up to 1500°C can produce either α -Si₃N₄ or β -Si₃N₄. As carbon is an active reducer of oxide, SiO₂ can also react with carbon directly to form SiC [18]. However, the formation of SiC can be avoided by controlling high pressure of nitrogen gas to promote the Si₃N₄ formation [19]. The overall reaction of the process can be described with the following reactions.



Nevertheless, the overall reaction is reported to be slow, requiring many hours to complete. As the reaction depends on solid contacts between silica and carbon, excess of carbon content is required for entire transformation of silica to silicon nitride, which often results in free carbon remaining in the nitrated powder. α -Si₃N₄ can be produced directly from very fine silica and carbon at temperature in the range of 1400 - 1500°C depending on the reactivity of raw materials. In some process, sintering additives such as MgO and Y₂O₃ were used for reduce the time to complete the reaction and change the morphology of product during sintering [20].

In some reports for the synthesis of α - Si_3N_4 via the carbothermal nitridation reaction, β - Si_3N_4 and SiC were by-products when the reaction conditions were changed. At the temperature higher than 1600°C , phase transformation from α - Si_3N_4 to β - Si_3N_4 will occur [21]. Besides, carbon reduces SiO_2 to pure silicon in this process and then pure silicon reacts with N_2 to form Si_3N_4 , while the impurity oxides of silica promote formation of β - Si_3N_4 instead of preferred α - Si_3N_4 [19]. $\text{Si}_3\text{N}_4/\text{SiC}$ nanocomposite powders were also synthesized via the carbothermal reaction of silica-phenol resin hybrid gels. The Si_3N_4 and SiC contents can be easily controlled by adjusting the reaction temperature and/or the starting carbon content, or using a two-stage process, while the size of the obtained Si_3N_4 particles can be effectively controlled by adding Si_3N_4 powder as seed particles to the silica/phenol resin gel [22].

The characteristics of the Si_3N_4 powder resulting from the carbothermal reduction process are affected by many factors such as silica-to-carbon molar ratio, nitrogen flow rate, reaction temperature, particle size and specific surface area of silica and carbon as well as the impurities. The carbothermal reduction and nitridation was used in this research because the porosity of silicon nitride can be controlled by porosity of carbon derived from phenol - resorcinol formaldehyde (PRF) gel.

2.3 Sol-Gel processing

Sol-gel process is a wet chemical technique for the fabrication of materials, including ceramics and organic-inorganic hybrids. It starts from chemical solution to produce a coordinated network, which is subjected to hydrolysis and polycondensation reactions to form colloidal suspension, or “sol” according to Equations 2.6 to 2.8, where M and R are metal atom and alkyl groups, respectively.



In general, the sol-gel process involves the transition of a system from liquid “sol” into solid “gel” phase. For the sol-gel process, it is possible to fabricate materials in a wide variety of forms, e.g. ultra-fine or spherical shaped powders, thin film coatings, ceramic fibers, porous or dense ceramic materials, monolithic ceramics and extremely porous aerogel materials as shown in Figure 2.4.

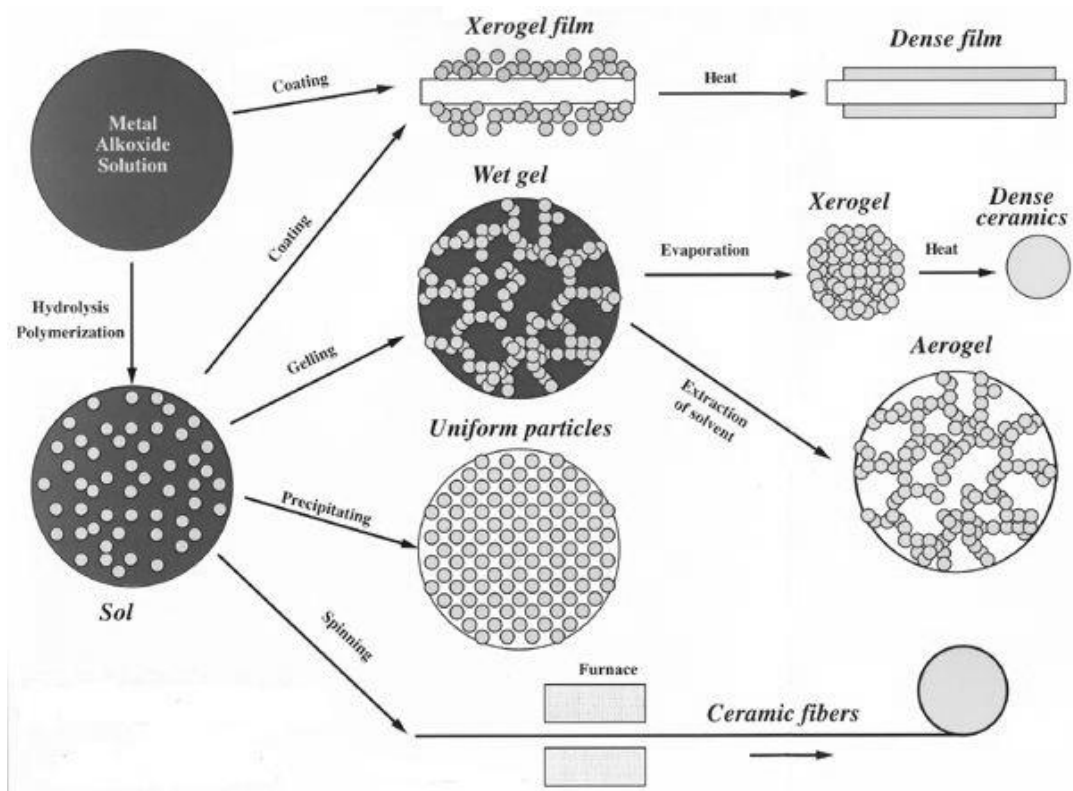


Figure 2.4 Sol-gel process and their products.

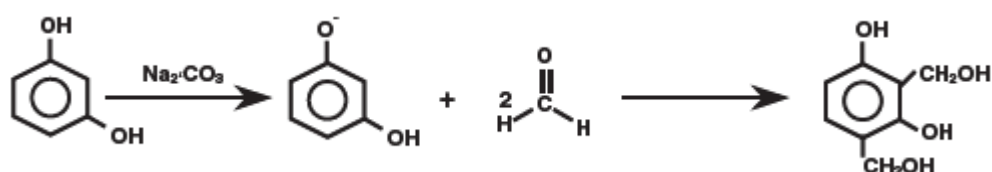
2.4 Resorcinol–formaldehyde (RF) gel

Organic and carbon aerogels were first produced by Pekala and co-workers. Their main research subject was resorcinol formaldehyde aerogels, but phenolic-furfurol or melamine-formaldehyde aerogels have also been produced and investigated [13].

Resorcinol–formaldehyde (RF) derived carbon gels are known as a source for excellent porous carbon materials due to their high specific surface area (400 – 1200 m²/g), high porosity (>80%), and large mesopore volume [23]. RF organic aerogels are useful precursors of carbon aerogels, which are consisted of solid carbon skeletons. They can be formed by pyrolysis of the RF gel in an inert atmosphere after solvent exchange and drying [24]. The obtain carbon gels are suitable for many applications such as adsorbents, column packing materials for high-performance liquid chromatography, electrode materials for electric double layer capacitors and catalyst supports [25].

The first RF gel was synthesized by Pekala via the sol-gel polycondensation of resorcinol (R) and formaldehyde (F) with sodium carbonate (C) as basic catalyst [12]. The intermediates formed during the reaction further react to form a cross-linked polymer network. The two major reactions include: (1) the formation of hydroxymethyl (-CH₂OH) derivatives of resorcinol, and (2) the condensation of the hydroxymethyl derivatives to form methylene (-CH₂-) and methylene ether (-CH₂OCH₂-) bridged compounds [26].

(1) Addition reaction



(2) Condensation reaction

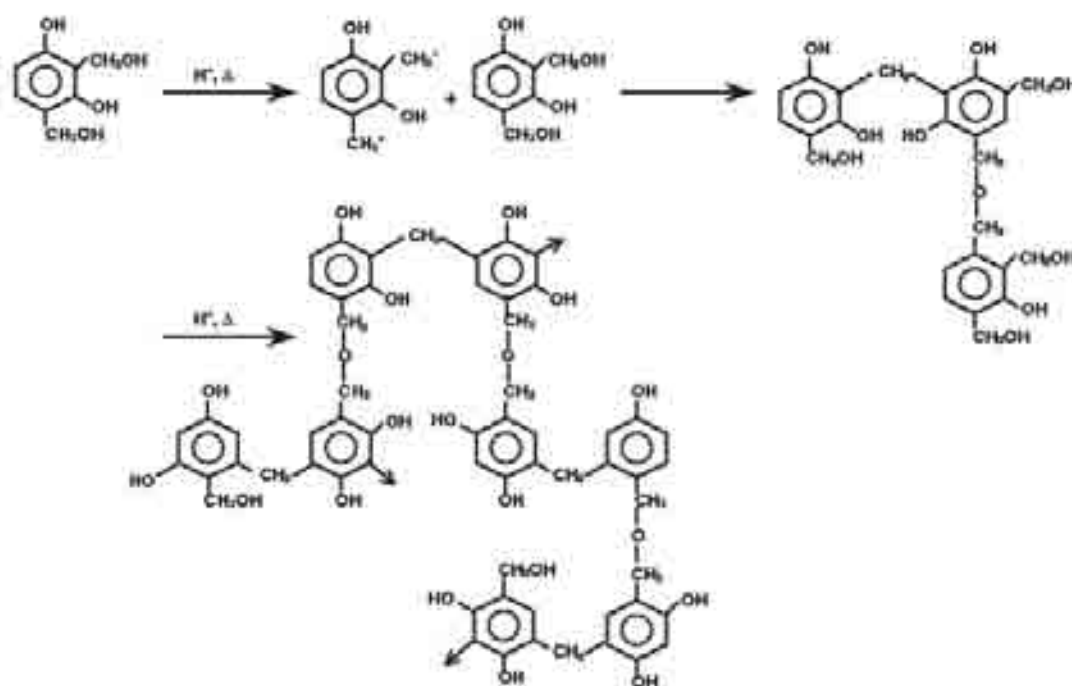


Figure 2.5 Molecular presentation of the polymerization mechanism of resorcinol with formaldehyde.

Porosity and surface area of the final products depend on the structure of their parent hydrogel, conditions of RF gel synthesis, drying conditions, and carbonizing techniques. A catalyst plays the most important role for the formation of the pore structure of the product. The catalyst initially promotes the generation of resorcinol anions. These anions are subsequently transformed into substituted resorcinol, which form RF clusters through polycondensation. Then RF clusters react with each other and grow into networks of colloidal particles, which finally form a RF hydrogel [27].

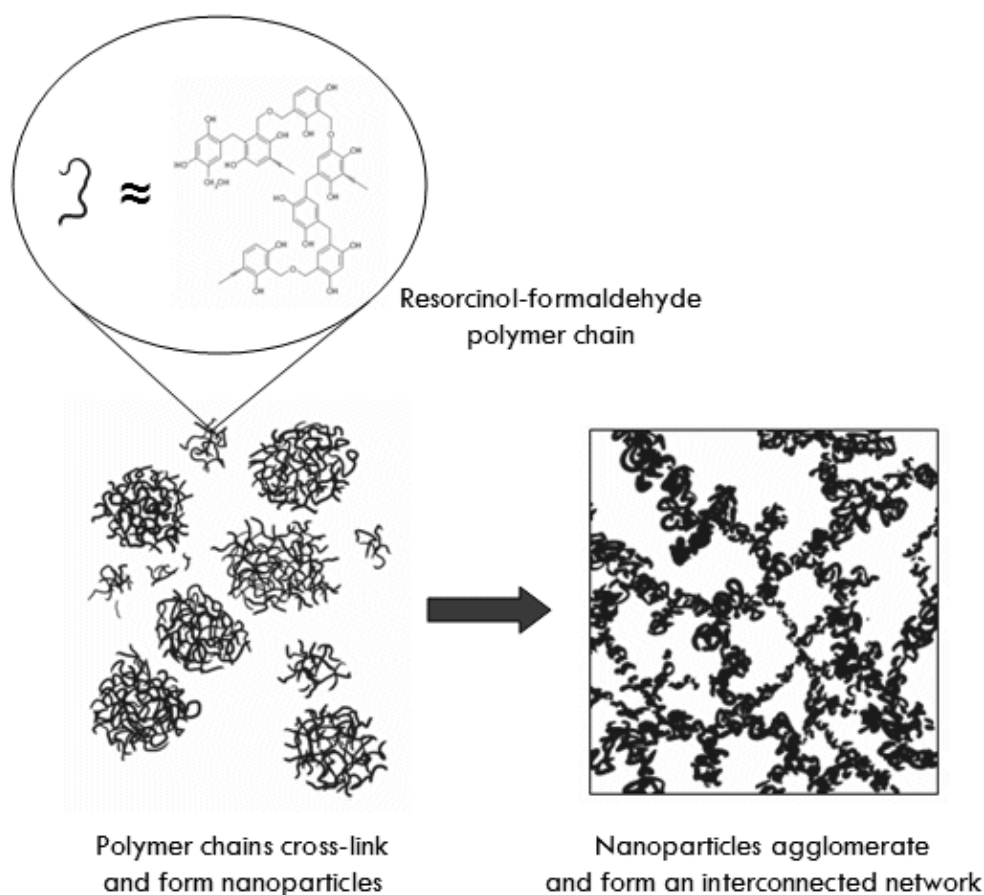


Figure 2.6 Gel formation in the resorcinol-formaldehyde system.

Thermal properties of RF gel were characterized by TGA and DTG. Three major weight losses were observed. The first weight loss was due to desorption of water at 150°C. The second weight loss was ascribed to desorption of organic molecule by breaking chemical bonds such as C–O at 400°C. The third weight loss was assigned to further carbonization reaction by breaking chemical bonds such as C–H at 600°C. The TGA analysis showed that there was no further weight loss above 800°C [28].

The technique of drying RF gels has effects on the structure of carbon gels. There are three kinds of drying methods commonly used to convert the hydrogel to a solid RF gel. The first method is drying in an inert atmosphere, which gives a RF xerogel with the lowest surface area (<900 m²/g) [29]. The second method is

extraction with supercritical CO₂, which gets a RF aerogel with an intermediate surface area (1000 m²/g) [30], and the final method is freeze-drying, which provides a RF cryogel with the highest surface area (>2500 m²/g) [25].

RF gel has been used as a template for the synthesis of porous silica. To form silica/RF gel, resorcinol and formaldehyde were used as a carbon source for porous RF structure and 3-aminopropyltrimethoxysilane (APTMS) was used as a silica precursor. The gel was formed via sol–gel polycondensation process. Pyrolysis of the dried gel at 250°C for 2 h following by at 750°C for 4 h resulted in silica/carbon composite which could be later converted into mesoporous Si₃N₄ or Si₃N₄/SiC composite via the carbothermal reduction and nitridation process at 1450°C. It was shown that the content of silica in the starting composite was an important factor influencing both phase and porosity of the product. The optimum SiO₂/C ratio of 0.05, was found to result in Si₃N₄ product with surface area as high as 212.63 m²/g. Moreover, the research demonstrated the effects of type of silica precursor i.e. 3-aminopropyltrimethoxysilane (APTMS), tetraethyl orthosilicate (TEOS) and sodium silicate, on how they affect the phase of Si₃N₄ products. It was found that APTMS was suitable to be used as silica precursor in the synthesis of α-Si₃N₄ from the silica/RF composite [31].

2.5 Phenol–formaldehyde (PF) gel

In general, organic and carbon aerogels were obtained through polycondensation of RF gel, solvent exchange, drying process, and finally carbonization under an inert atmosphere. However phenol-formaldehyde (PF) gel was also an alternative starting material for the synthesis of carbon aerogels under similar procedure of RF gel [13]. If phenol is considered as the substitution for resorcinol, the reaction scheme should be very similar to Figure 2.7, because both monomers possess a negative electron charge at 2,4,6-ring position, regardless of the lack of one of the hydroxyl-groups in case of phenol that leads these positions to a reduced electron density compared to resorcinol. As a consequence, the solubility of phenol in water

(80 g/l) is drastically reduced compared to resorcinol (500 g/l) [32] and the reactivity of phenol is about 10–15 times lower than the reactivity of resorcinol [33]. Therefore the phenol content in the starting aqueous solution is limited to small values, because otherwise segregation will take place.

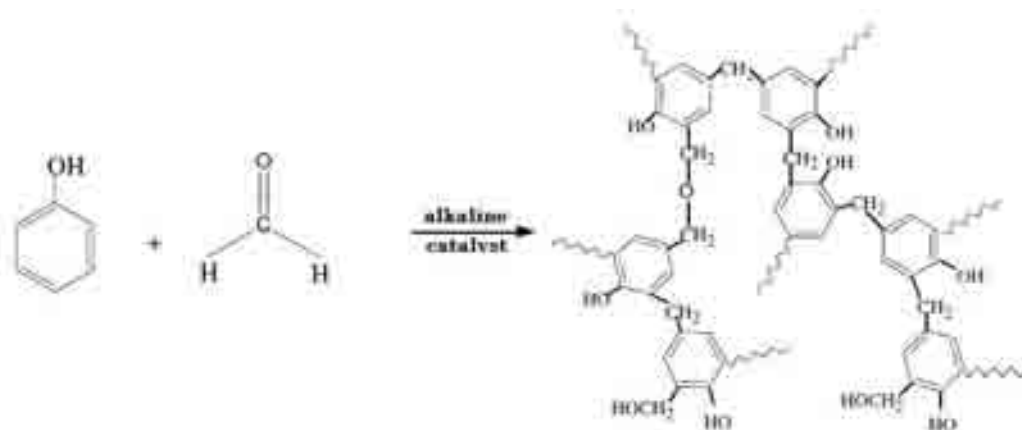


Figure 2.7 A schematic diagram of the reaction of phenol and formaldehyde catalyzed by alkaline catalyst.

It should be noted that, acid catalysts have less ability to achieve a high crosslink density than base catalysts [34]. Moreover, phenol behaves like weak acids and thus reacts rapidly with alkali (e.g. NaOH) to form phenoxide ion, whose oxide group, as a very strong activating substituent, has great ability in increasing the electron density in the 2, 4, 6 ring positions [35]. Therefore, based upon these facts, it is believed that phenol can also undergo the sol–gel polymerization with formaldehyde in much the same manner as resorcinol under proper alkaline catalyst conditions. Nevertheless, phenol requires a significantly higher catalyst concentration to increase the reaction rate.

For the formation of PF gel, phenol reacts with formaldehyde under alkaline conditions to form mixture of addition and condensation compounds, which can react further to form a hydrogel network. It is credible that the sol–gel polymerization of phenol with formaldehyde includes two principal reactions: (1) the formation of hydroxymethyl derivatives ($-\text{CH}_2\text{OH}$) of phenol; (2) the condensation of

hydroxymethyl derivatives to form methylene (-CH₂-) and methylene ether bridged compounds (-CH₂OCH₂) [35].

The thermal properties of PF gel were characterized by TGA and DTG. The initial mass loss was due to the loss of the water content at 118°C. The second mass loss was attributed to the breakdown of methylene linkages to yield aldehydes and phenols at 475°C. Finally, about 30% of the mass remains as a coke-like solid mass residue above 600°C [36]. When compared to the RF gel, it was indicated that the oxidation of carbon derived from RF and PF gels was found to occur at different temperature although the structures of RF and PF gel were similar. However, it was found that specific surface area and pore volumes of PF gel were less than RF gel. PF gel had a narrow range which from 300 to 700 m²/g and 0.08 to 1.84 cm³/g, respectively.

It is possible to obtain low density carbon aerogels from organic gels derived via the polycondensation reaction of phenol and formaldehyde (PF) in aqueous, using base catalysed system [37,38], but their process still requires solvent exchange and freeze drying or supercritical ethanol drying. Phenol could undergo the sol-gel polymerization with formaldehyde to form organic gels when the great amount of NaOH is used as catalyst, followed by ethanol supercritical drying to prepare low-density organic and carbon aerogels. Synthesis conditions, such as the P/C ratio, the P/F ratio, PF content and gelation temperature, play a significant role in the fabrication of low-density organic and carbon aerogels. The framework of the phenol derived organic and carbon aerogels was similar to that of typical resorcinol-formaldehyde aerogels obtained with CO₂ supercritical drying technique. The networking particles of the aerogels obtained were approximately 10–15 nm in diameter, which defined numerous mesopores smaller than 50 nm. As a result, the highest measured BET surface area and mesopore volume of the carbon aerogels obtained reached 714 m²/g and 1.84 cm³/g, respectively [38]. Moreover, sodium carbonate could also be used as the catalyst to prepare PF carbon cryogels. The mixture was aged and the water in the obtained samples was exchanged with *t*-butanol, followed by freeze drying. The obtained PF cryogels were carbonized at

1000°C for 4 h in a nitrogen atmosphere and were transformed to PF carbon cryogels. The BET surface area of this sample was 400 m²/g, and its micropore volume and mesopore volume were 0.08 cm³/g and 1.2 cm³/g, respectively [37].

CHAPTER III

EXPERIMENTAL

This chapter describes the experimental procedures used in this research. It is divided into five sections: chemicals, preparation of silica/PRF gel, preparation of silica/carbon composite, carbothermal reduction and nitridation of silica/carbon composite and characterizations of the products.

3.1 Chemicals

Phenol (P) > 99%, resorcinol (R) 99.8% and formaldehyde (F) 37% aqueous solution were used to prepare PRF gel. Sodium carbonate anhydrous (Na_2CO_3) 99.8% was used as a catalyst for PRF gel preparation. 3-Aminopropyltrimethoxysilane (APTMS) 97% was used as a precursor of silica.

Phenol, resorcinol, formaldehyde solution, and sodium carbonate anhydrous were purchased from Asia Pacific Specialty Chemicals Limited. APTMS was purchased from Sigma-Aldrich Chemical Company. All chemicals were used as received without further purification.

3.2 Preparation of silica/PRF gel

Phenol (P) and resorcinol (R) were firstly dissolved into DI water (W) and stirred until the dissolution was completed. Next, sodium carbonate (C) was added into the solution and stirred at room temperature for 15 min. After that, formaldehyde solution was added, using R/F molar ratio of 0.5, R/W molar ratio of 0.15 and C/W ratio of 10 mol/dm^3 and stirred for 15 min. Then, APTMS in the predetermined amount was added to the solution under continuous stirring at room temperature. The

mixture was aged at the room temperature without stirring for 3 days. After aging, solvent in the gel was removed by solvent exchange process, i.e., the sample was immersed in *t*-butanol for 24 h, renewed with fresh *t*-butanol everyday. The solvent exchange process was repeated for three times. Finally, the obtained gel was removed from *t*-butanol and dried in freeze drying process at -40°C for 3 days to obtain dried silica/PRF gel.

3.3 Preparation of porous silica/carbon composite

Porous silica/carbon composite was obtained by pyrolysis of the dried silica/PRF gel in the step-wised fashion. The dried gel was heated under continuous flow of nitrogen gas (25 ml/min) in a tubular flow reactor operated at 250°C for 2 h and subsequently heated up to 750°C and held for another 4 h. The heating rate employed was fixed at $10^{\circ}\text{C}/\text{min}$. Finally, it was calcined in a box furnace at the controlled calcination temperature in the range of 400 to 500°C for 2 h to partially remove carbon from the composite. The product of this step is porous silica/carbon composite.

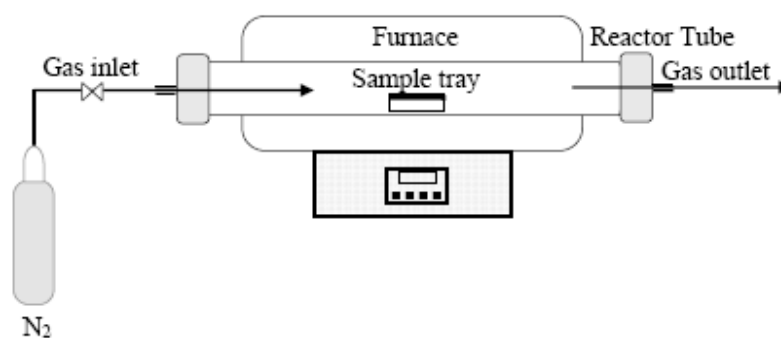


Figure 3.1 Schematic diagram of the tubular flow reactor used for the preparation of silica/carbon composite.

3.4 Carbothermal reduction and nitridation of silica/carbon composite

In the carbothermal reduction and nitridation process, the silica/carbon composite was put into an alumina tray (25 mm x 15 mm x 5 mm deep) and placed in a horizontal tubular flow reactor. The schematic diagram of the reactor system is shown in Figure 3.2. The composite was then heated to 1450°C using the heating rate of 10°C/min under a continuous flow of argon at 50 l/h. After the temperature had reached 1450°C, the gas stream was switched from argon to a mixture of 90% nitrogen and 10% hydrogen with same total flow rate. The reaction was held at constant temperature for 10 h. The obtained product was subsequently calcined in a box furnace at 800°C for 8 h to remove the residual carbon.

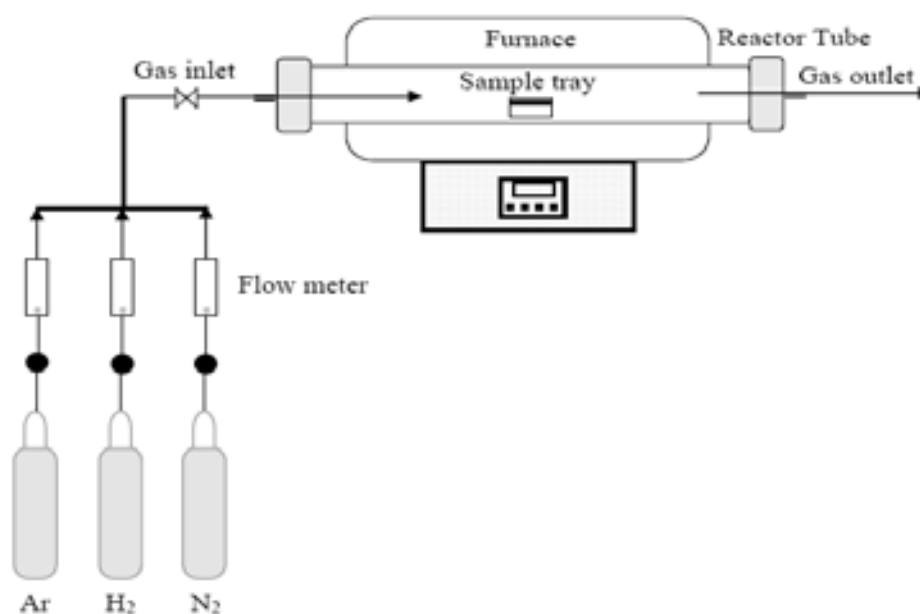


Figure 3.2 Schematic diagram of the tubular flow reactor used for the carbothermal reduction and nitridation.

3.5 Characterizations of the products

The obtained products were characterized by using various techniques, as following:

3.5.1 X-ray diffraction analysis (XRD)

Crystalline phases of the product were determined from X-ray diffraction analysis, using a SIEMENS D5000 diffractometer with $\text{CuK}\alpha$ radiation. Each sample was scanned in the range of $2\theta = 10\text{-}50^\circ$ with a step size of $2\theta = 0.02^\circ$.

3.5.2 Fourier-transform infrared spectroscopy (FT-IR)

The functional groups in the samples were determined by using a Fourier transform infrared spectrometer (Nicolet 6700) at Center of Excellence in Particle and Technology Engineering laboratory, Chulalongkorn University. The spectra were recorded at wavenumber between 400 and 4000 cm^{-1} with resolution of 2 cm^{-1} . The number of scan for the measurement was 64. The sample was mixed with KBr with the sample to KBr ratio of 1:100 and formed into a thin pellet, before measurement.

3.5.3 Scanning electron microscopy (SEM)

Morphology of the products was examined by using a scanning electron microscope (JSM-6400, JEOL Co., Ltd.) at the Scientific and Technological Research Equipment Center (STREC), Chulalongkorn University.

3.5.4 Transmission electron microscopy (TEM)

Morphology of an individual grain in the samples was observed on a JEOL JEM-2100 Analytical Transmission Electron Microscope, operated at 80-200 keV at the Scientific and Technological Research Equipment Center (STREC), Chulalongkorn University. The crystallographic information was also obtained from the selected area electron diffraction (SAED) analysis performed in the same instrument.

3.5.5 Surface area measurement

The specific surface area of products was determined via nitrogen adsorption/desorption analysis using the Brunauer-Emmett-Teller (BET) model, by Belsorp mini II BEL, Japan at Center of Excellence in Particle and Technology Engineering laboratory, Chulalongkorn University.

3.5.6 Thermogravimetric analysis (TGA)

The residual carbon content and thermal behavior of the samples were determined by using thermogravimetric analysis on a Mettler-Toledo TGA/DSC1 STARe System at Center of Excellence in Particle and Technology Engineering laboratory, Chulalongkorn University. The analysis was performed from temperature of 25 to 1,000°C under a heating rate of 10°C/min in 40 ml/min flow of either oxygen or nitrogen.

CHAPTER IV

RESULTS AND DISCUSSION

In this chapter, silica/PRF gels, pyrolyzed silica/PRF composites and nitrated products fabricated by combined sol-gel method and carbothermal reduction and nitridation technique are investigated. Effects of various factors, such as composition of the PRF-gel, silica-to-carbon molar ratio of the composites, controlled calcination temperature, as well as the use of pre-formed silica sol as source are presented.

In the first section, the overall process and the overall results were described. First of all, silica/PRF composite was prepared by the method as mentioned earlier. Next, the silica/PRF composite was pyrolyzed under nitrogen gas to convert the PRF structure into porous silica/carbon composite and then it was calcined in a box furnace at the controlled calcination temperature to partially remove carbon from the composite. Finally, the silica/carbon composite was subjected to the carbothermal reduction and nitridation process at 1450°C for 10 hours followed by the removal of excess carbon by calcination at 800°C for 8 hours.

Figure 4.1 shows SEM micrographs of the product after different preparation steps. It can be seen the products obtained after pyrolysis, after being calcination and after being nitrated (Figure 4.1(a)-(c)) have similar morphology, all of which are consisting of spherical grains with uniform size. The result indicates that the structure, morphology as well as porosity of subsequent products depend upon the formation of silica/PRF gel. BET surface area of the pyrolyzed silica/carbon after the first calcination (377 m²/g) is high because the composite still contains high carbon content. After the nitridation process, the surface area is dramatically decreased (135 m²/g), which is a result from the fact that some carbon in the product was used in the carbothermal reduction and nitridation process. Moreover, the final product after the final calcination (Figure 4.1(d)) has different morphology than the products from other preparation step. It has much lower surface area (75 m²/g) than the nitrated

product because the residual carbon was burned out leaving only silicon nitride in the product. Therefore, it can be concluded that the residual carbon in the sample contributes to large fraction of the measured surface area.

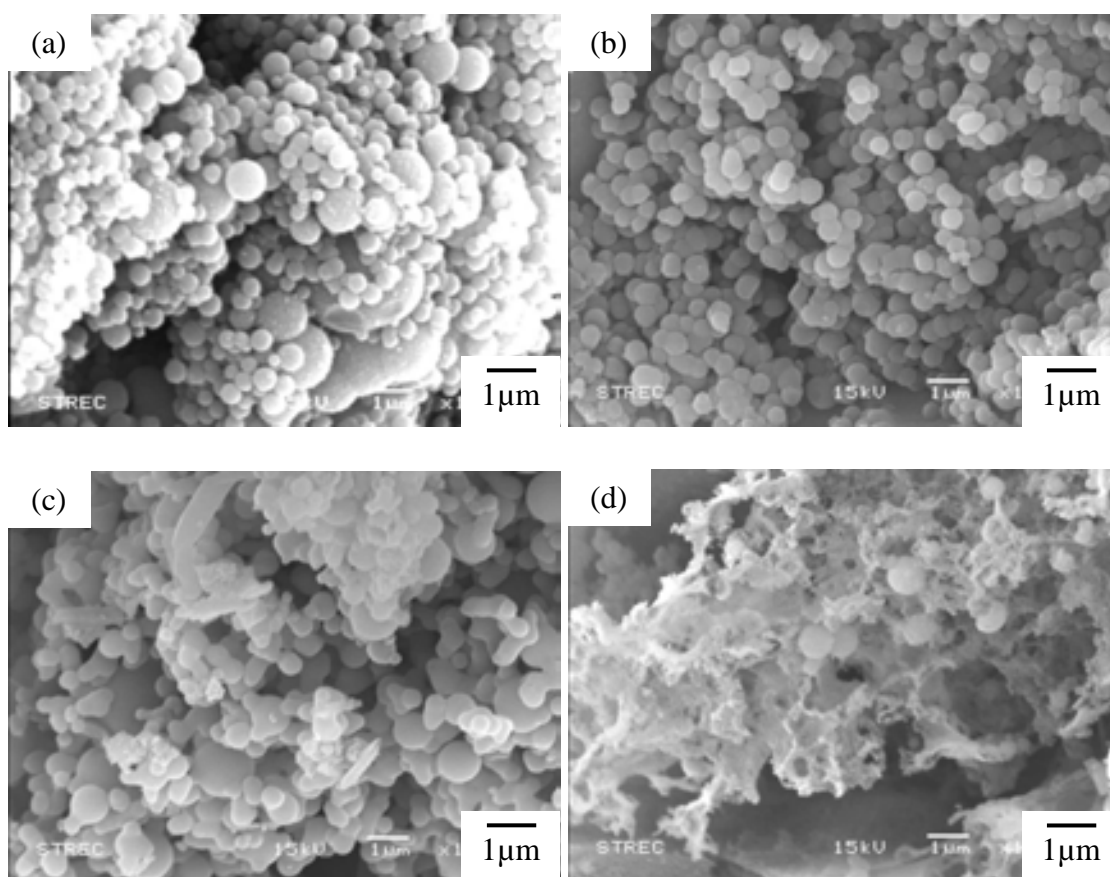
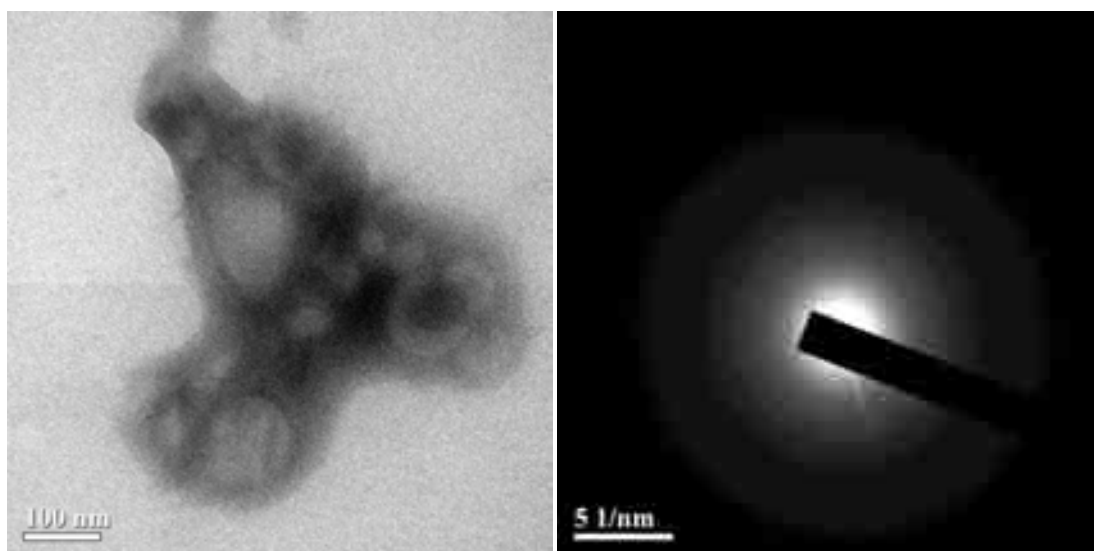


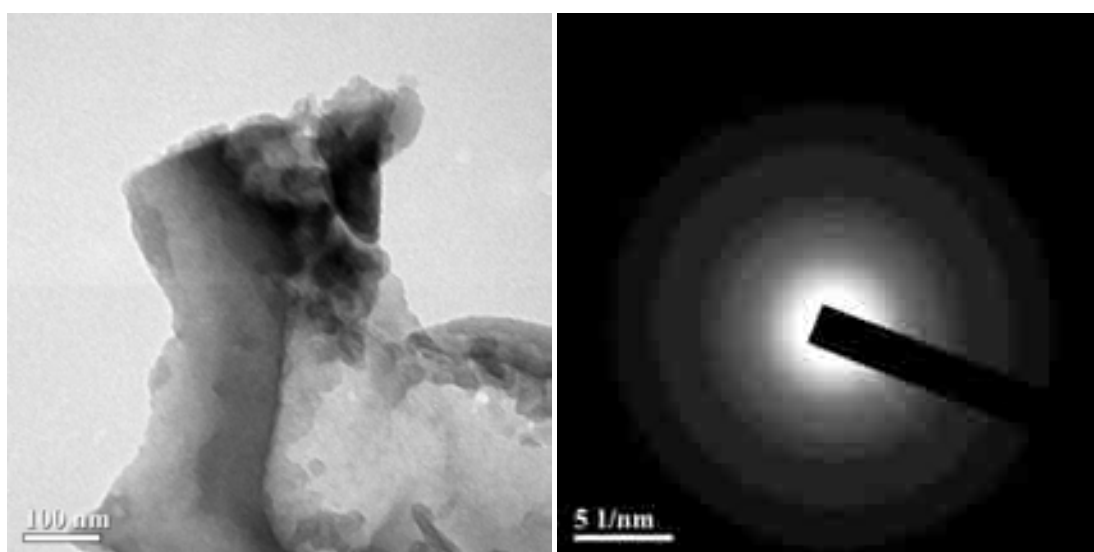
Figure 4.1 SEM micrographs of silica PRF composite prepared by using P/R molar ratio of 0.5 and the SiO_2/C molar ratio of 0.05: (a) after pyrolysis (b) after pyrolysis and first calcination, (c) after nitridation and (d) after final calcination.

TEM micrographs and SAED patterns of the product after different preparation steps are shown in Figure 4.2 and 4.3. Both of silica/PRF composites before and after being pyrolyzed have amorphous phase as shown in SAED analysis in Figure 4.2 (a) and 4.2 (b). On the contrary, the TEM micrographs and SAED patterns of both the nitrided product and the product after final calcination reveal

crystal phase, as confirmed by the SAED patterns in Figure 4.3 (a) and 4.3 (b), respectively. However, the final product after calcination has higher crystallinity than the product obtained right after being nitrided, as evidenced from the SAED patterns shown in both Figure 4.3 (a) and (b). According to the TEM micrographs of the product after the final calcination process (Figure 4.3), the particles of silicon nitride product are agglomerated and the particles size is around 50 nm.

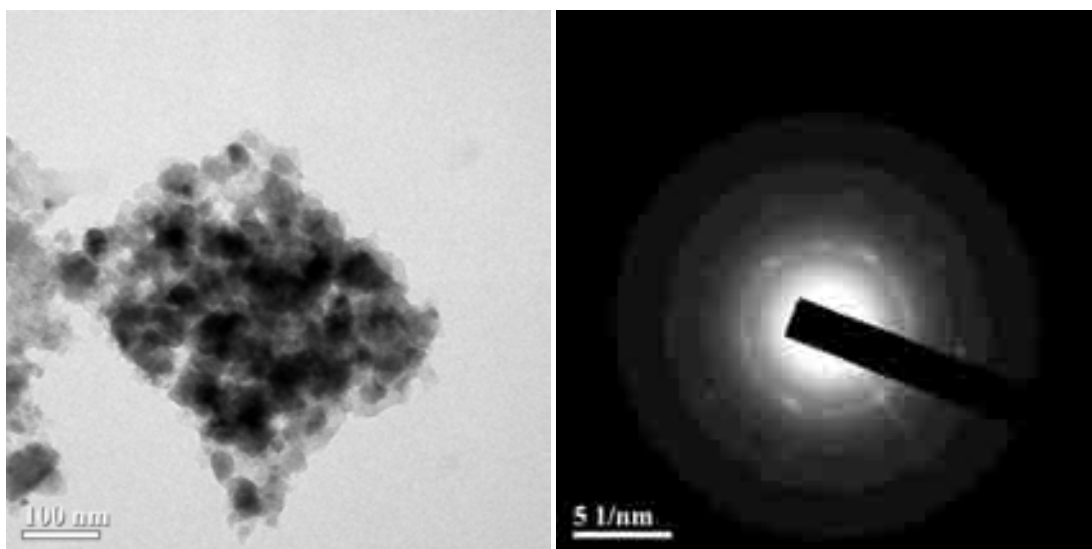


(a)

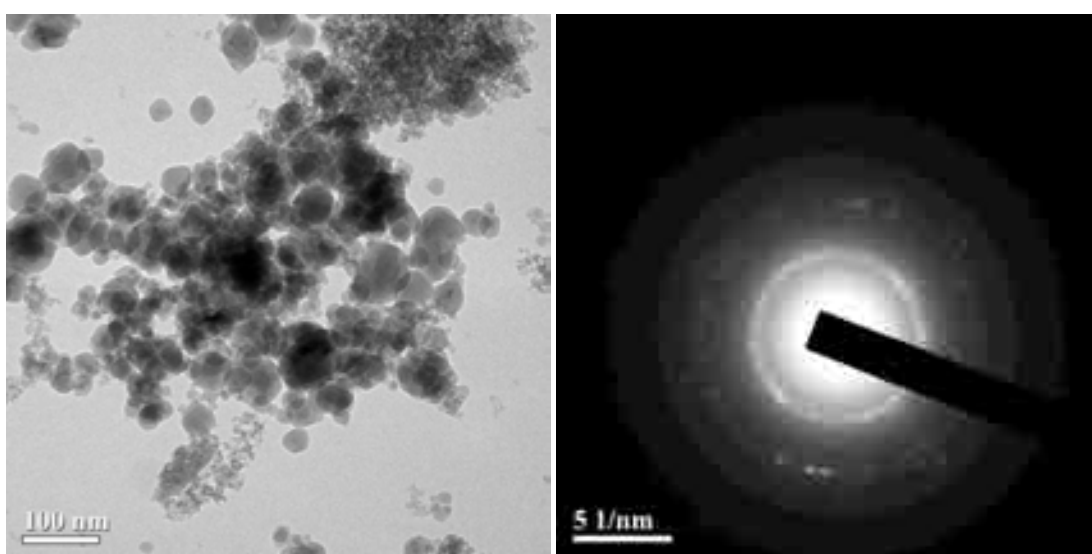


(b)

Figure 4.2 TEM micrographs and SAED patterns of silica/PRF composite prepared by using P/R molar ratio of 0.5 and the SiO_2/C molar ratio of 0.05: (a) before pyrolysis and (b) after being pyrolysis and first calcination.



(a)



(b)

Figure 4.3 TEM micrographs and SAED pattern of silica/PRF composite prepared by using P/R molar ratio of 0.5 and the SiO_2/C molar ratio of 0.05: (a) after nitridation and (b) after final calcination.

Figure 4.4 shows result from X-ray diffraction analysis of the product after final calcination. The sample was prepared by using P/R molar ratio of 0.5 and SiO_2/C molar ratio of 0.05. According to the XRD analysis, it indicates that the final product is α -phase of silicon nitride. The average crystallite size of the product is around 43 nm, which was calculated from the width at half-height of peak at the (201) plane of α -silicon nitride using the Scherrer equation. The result corresponds with the average particle size measured by TEM micrograph (Figure 4.3), which suggests that the silicon nitride product is single crystal. However, this figure shows the collection of single crystal of silicon nitride.

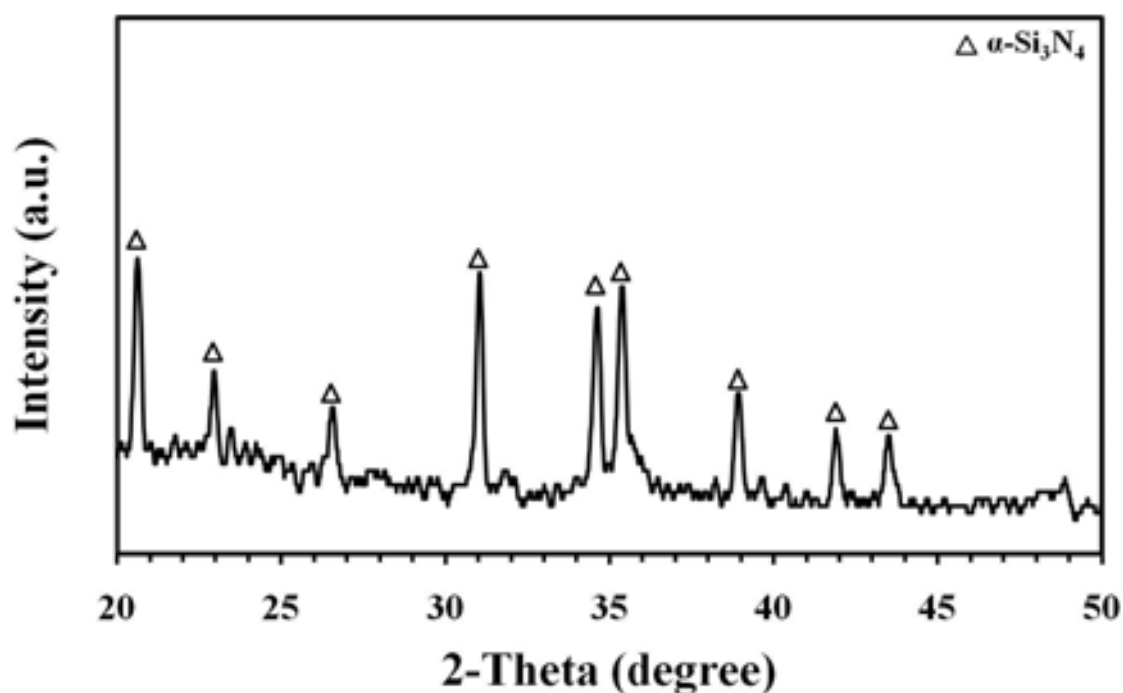


Figure 4.4 XRD patterns of silicon nitride product, after calcination at 800°C for 8 h. The products were synthesized with P/R molar ratio of 0.5 and SiO_2/C molar ratio of 0.05.

4.1 Effect of phenol-to-resorcinol molar ratio

The effect of phenol-to-resorcinol (P/R) molar ratio is investigated in this section. All samples were prepared by using R/F, R/W, SiO₂/C molar ratios of 0.5, 0.15 and 0.05, respectively. Figure 4.5 shows FTIR spectrum of dried silica/PRF gels prepared using various P/R molar ratios. All samples show similar main functional groups. The absorption bands at wave number of 696 and 1100 cm⁻¹ are corresponding to symmetric bending and antisymmetric stretching vibrations of Si–O–Si bonding [39], respectively, which confirm the presence of silica in all composites. The signal at wavenumber around 450 cm⁻¹ is indicated as the deformation vibration of O–Si–O group [40]. Other signals are associated with PRF gel. The absorption band at 1102 cm⁻¹ represents asymmetric stretching vibration of C–O–C aliphatic ether, while that located at 1444 cm⁻¹ is assigned to –CH₂– scissor vibration in methylene bridge [41]. It should be noted that the –CH₂– bonding is a result from a bridge between two aromatic rings, formed by the interaction of hydroxymethyl derivatives of resorcinol [42]. The band at 1218 and 1220 cm⁻¹ are corresponding to C–C–O asymmetric stretching vibration. Finally, the IR band at 1615 cm⁻¹ is assigned to C=C stretching vibration in aromatic rings [41]. All FT-IR bands that have been proposed to associate with the functional groups of dried silica/PRF gel prepared by using various P/R molar ratios are shown in Table 4.1.

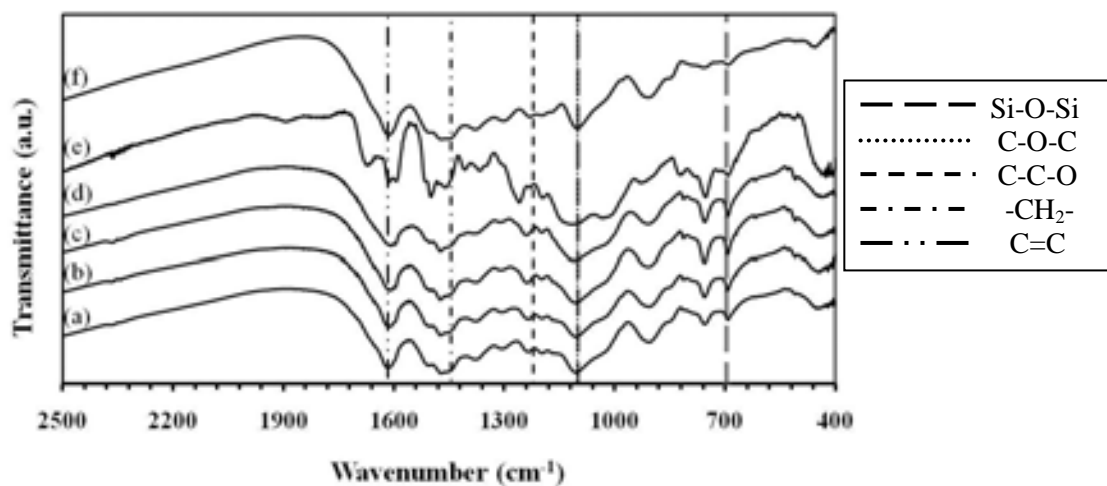


Figure 4.5 FTIR spectrum of dried silica/PRF gel prepared by using P/R molar ratio of 0.3 (a), 0.5 (b), 1.0 (c), 1.5 (d), compared with that of silica/PF gel (e), and silica/RF gel (f).

Table 4.1 Assignments of FTIR absorption bands of the dried silica/PRF gels.

IR bands (cm^{-1})	Functional groups
1615	C=C stretching vibration in aromatic rings [41]
1444	-CH ₂ - scissor vibration in methylene bridge [41]
1220, 1218	C-C-O asymmetric stretching vibration [41]
1102	C-O-C asymmetric stretching vibration of aliphatic ether [41]
1100	Si-O-Si bonding antisymmetric stretching vibration [39]
696	Si-O-Si bonding symmetric bending vibration [39]
450	O-Si-O deformation vibration [40]

Figure 4.6 shows morphologies of pyrolyzed silica/carbon composites observed with SEM. It is clearly seen that most of the pyrolyzed composites have same morphology which appears to be agglomerated spherical particles. It is also shown that the molar ratio of P-to-R affects the uniformity of the pyrolyzed particles. According to the SEM images, size of the particles is uniform in the pyrolyzed silica/PF composite and pyrolyzed silica/RF composite (Figure 4.6 (e-f)). On the other hand, size of particles in the sample of pyrolyzed silica/PRF composites is not uniform (Figure 4.6 (a-d)). The difference in particle size depends on the nature of precursors. For instance the solubility of phenol in water is drastically reduced comparing to that of resorcinol [32] and the reactivity of phenol is about 10–15 times lower than the reactivity of resorcinol [33]. Thus, non-homogeneous mixing between resorcinol and phenol within the silica/PRF gel has an effect on particle size with that of silica/carbon composite.

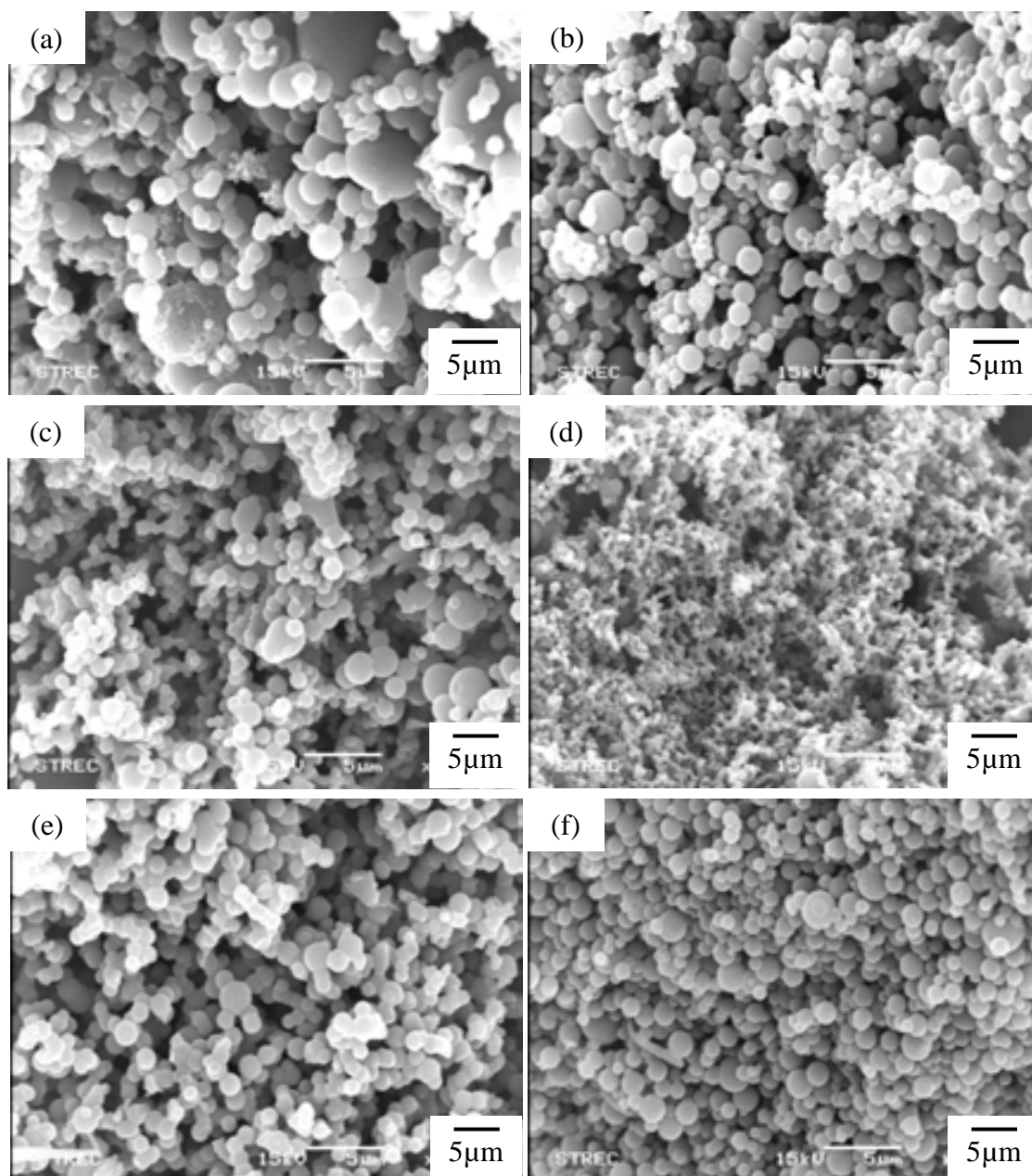


Figure 4.6 SEM micrographs of pyrolyzed silica/PRF composites. The composites were prepared by pyrolysis of silica/PRF gels using P/R molar ratio of 0.3 (a), 0.5 (b), 1.0 (c), 1.5 (d), compared with that of pyrolyzed silica/PF composite (e), and pyrolyzed silica/RF composite (f).

Table 4.2 shows BET surface area and carbon content of the pyrolyzed silica/PRF composites with various molar ratios of P-to-R after being calcined at 500°C for 2 h. From the results, it is found that the surface area of silica/carbon composite is generally increased with the increasing phenol content, but the P/R molar ratio of 1.0 result in the silica/carbon composite with the highest surface area (536.7 m²/g). For the pyrolyzed silica/PF gel and pyrolyzed silica/RF gel, surface areas of the two silica/carbon composites are similar but less than that of the pyrolyzed silica/PRF composite. This is because when the silica/PRF composite, which was mixed from two precursors (i.e., phenol, resorcinol), was subjected to the pre-calcination process, carbon derived from different precursor was partially removed at different time. It results in the higher surface area of the silica/PRF composite. According to the TGA results, the content of carbon remaining in the composites is inversely relating to the specific surface area. It is suggested that the enhanced surface area is a result from the loss of carbon derived from part of the PRF-gel in the composites. Adding phenol to the RF gel to form PRF composite is advantageous because it enhances porosity of the composite after pre-calcination process, which consequently results in increasing porosity of the silicon nitride product.

Table 4.2 Specific surface area and carbon content of pyrolyzed silica/PRF composites after being calcined at 500°C for 2 h. The composites were prepared by pyrolysis of silica/PRF gels synthesized with various molar ratios of P-to-R, compared with that of pyrolyzed silica/PF gel, and pyrolyzed silica/RF gel.

P/R Molar ratio	Silica/carbon composite after calcination at 500°C for 2h	
	Surface area	Carbon content
	(m ² /g)	(%)
0.3	435.5	50
0.5	530.4	45
1.0	536.7	37
1.5	517.3	43
Neat P	437.5	49
Neat R	459.6	48

Pore size distributions of the pyrolyzed silica/PRF composites after being calcined at 500°C for 2 h are shown in Figure 4.7. All samples were prepared with SiO₂/C molar ratio of 0.05, various molar ratios of P-to-R. It can be seen that almost all samples are mesoporous carbon with a narrow pore size distribution around 3.5 nm and share common feature in the distribution. The only exception is the one prepared with neat PF gel, which shows pore size in the range of micropore (inset).

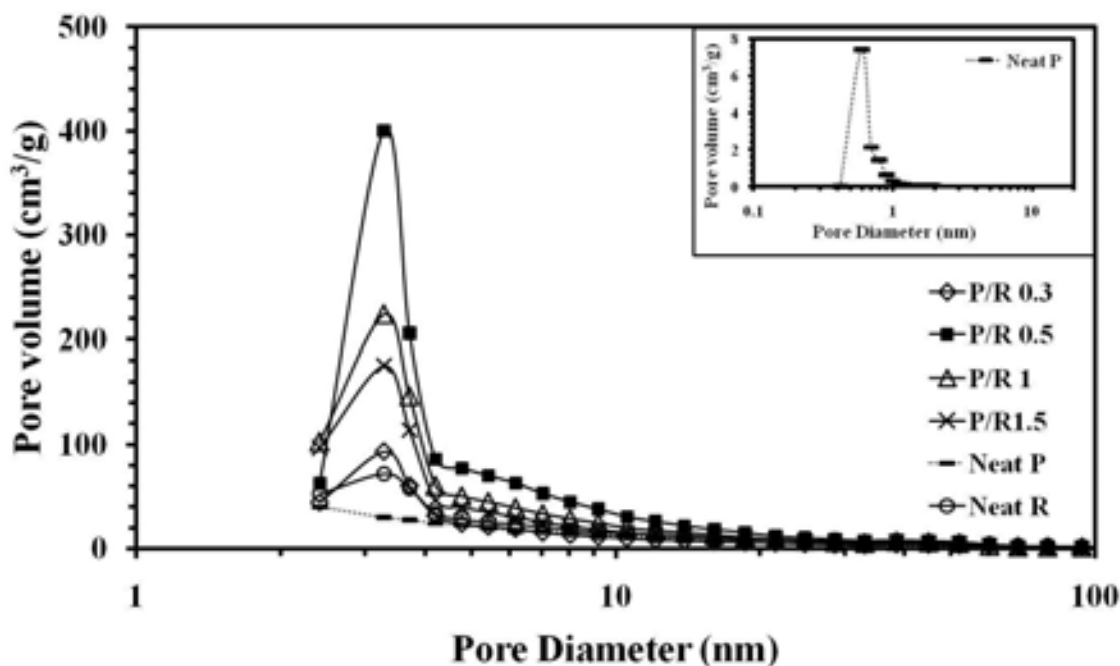


Figure 4.7 Pore size distribution of pyrolyzed silica/PRF composites after being calcined at 500°C for 2 h. The composites were prepared by pyrolysis of silica/PRF gels synthesized with various molar ratios of P-to-R.

Table 4.3 shows the results for the thermal degradation analyses of the silica/PRF gel and pyrolyzed silica/PRF composite (i.e., silica/carbon composite). The analysis of the silica/PRF gel was done in nitrogen, which simulated the pyrolysis process in the step-wised fashion at 250°C to 750°C. In the process, silica/PRF gel was converted to silica/carbon composite. The results indicate that about 48-60 wt% of organic compound was lost during the pyrolysis. On the other hand, the analysis of the pyrolyzed composite was done in oxygen in the range from 25°C to 1000°C to measure amount of carbon in the composite. The results suggest that the content of silica in the composite is in the range of 26-47 wt% and the rest is residual carbon in the sample. Nevertheless, the most important finding is that the silica/carbon composite prepared from silica/PF gel shows higher thermal stability than that derived from silica/RF gel. In the other words, addition of phenol into the gel results in stronger structure.

Table 4.3 TGA analysis of the samples after being freeze-dried (silica/PRF gel) and after being pyrolyzed (i.e., silica/carbon composites), prepared using various P-to-R molar ratios. The SiO₂/C molar ratio was fixed at 0.05.

Sample	% Mass loss	
	Silica/PRF gel	Silica/carbon composite
	(N ₂ atmosphere)	(O ₂ atmosphere)
neat R	62	74
P:R 0.3	49	53
P:R 0.5	51	64
P:R 1.0	52	57
P:R 1.5	48	58
neat P	49	53

In the carbothermal reduction and nitridation process, the silica/carbon composite was heated to 1450°C and held for 10 h under nitrogen and hydrogen flow. The obtained product was subsequently calcined in a box furnace at 800°C for 8 h to remove the residual carbon. The results from the X-ray diffraction (XRD) analysis revealed that all of the final products after the final calcination to remove excess carbon are crystalline, mainly Si₃N₄ in α -phase, as shown in Figure 4.8. However, signals corresponding to β -phase of Si₃N₄ and β -phase of SiC are also detected in the products synthesized with P/R molar ratios of 1.0 and 1.5 as well as those from silica/PF composite and silica/RF composite (Figure 4.8(c)-(f)). It is generally considered that SiC is formed by the reaction of gaseous silicon monoxide (SiO) and carbon monoxide (CO) or carbon (C) in the carbothermal reduction and nitridation process [43]. In addition, from the intensity of the signals, it is found that the sample prepared with silica/PF composite (Figure 4.8(e)) has lower crystallinity than the others. It can be seen that carbon precursor has an effect on the formation of crystalline silicon nitride. The average crystallite sizes, which were determined using the Scherrer equation, are shown in Table 4.4. Although the product consists of multiple phases, purification is not necessary because the product will be sintered at high temperature before being used in many applications. During the sintering

process, α -phase of Si_3N_4 will transform to β -phase, leaving only β - Si_3N_4 and β -SiC in the product.

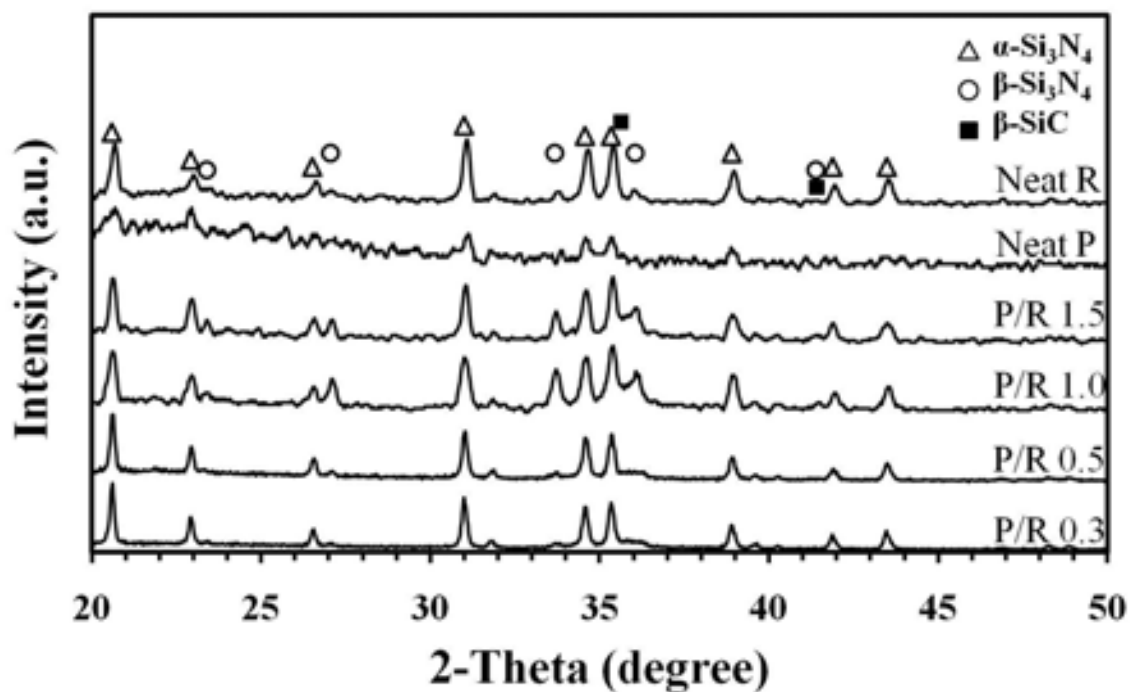
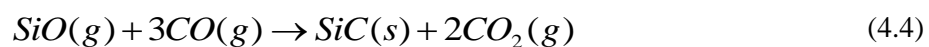
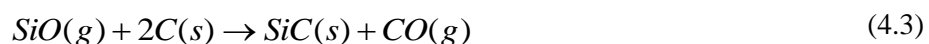
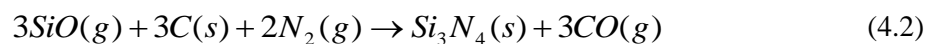
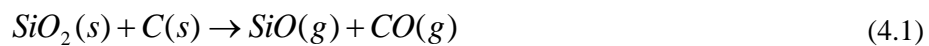


Figure 4.8 XRD patterns of silicon nitride powder, after the final calcination at 800°C for 8 h. The products were synthesized with P/R molar ratios of 0.3 (a), 0.5 (b), 1.0 (c), 1.5 (d), compared with that synthesized from silica/PF composite (e), and silica/RF composite (f). The SiO_2/C molar ratio was fixed at 0.05.

Table 4.4 Crystallite sizes of silicon nitride powder, after the final calcination at 800°C for 8 h. The products were synthesized from silica/PRF composites with various molar ratios of P-to-R.

P/R Molar ratio	Average crystallite size (nm)
0.3	35.6
0.5	33.4
1	29.2
1.5	44.7
Neat P	39.4
Neat R	39.8

The mechanism of formation of silicon nitride synthesized via the carbothermal reduction and nitridation process has been proposed earlier [18]. Usually, the carbothermal reaction according to reactions (2.1) and (2.2) take place at temperature above 1400°C, and these reactions are believed to involve multiple steps. First of all, according to reaction (4.1), the reductions of SiO₂ into SiO vapor by carbon in direct physical contact with SiO₂. Then, the silicon nitride product was formed through reaction (4.2). Some of gaseous SiO reacts directly with carbon or carbon monoxide to form SiC via reaction (4.3) and (4.4). From these mechanisms, it should be noted that the SiO₂/C composite can produce both Si₃N₄ and SiC.



The surface areas of the products, after the final calcination to remove residual carbon are shown in Table 4.5. It is seen that surface area of all products synthesized in this section is one order of magnitude higher than that of the conventional silicon nitride (1.2-13.0 m²/g)*. The surface area of the final product, which was pre-calcined at 500°C for 2h, reached maximum in the silica/RF composite (146.8 m²/g with 8% residual carbon). On the other hand, the surface area of the final product, which were pre-calcined at 400°C and 450°C for 2h, reached maximum in the silica/PF composite (420.4 and 395.6 m²/g with 7% and 5% residual carbon, respectively). The results from TGA analysis in oxygen suggest that majority of the residual carbon can be removed by calcination. Only small amount the remaining of carbon in the product after calcination is observed. The sample prepared with P/R molar ratio of 1.0 shows slight mass increase (-2.07 % wt of mass loss), which is the result from surface oxidation of silicon nitride to form SiO₂ according to reaction (4.6) [15]. It is suggested that, at this P-to-R molar ratio, it has no residual carbon left in the product and the surface area (82 m²/g) measured in this sample is indeed the area of Si₃N₄ products, not the residual carbon.

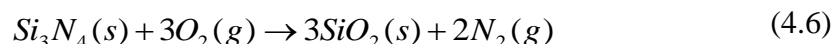


Table 4.5 Surface area and % mass loss from TGA analysis in oxygen atmosphere of silicon nitride products after final calcination. The composites were prepared from SiO₂/PRF gel with various molar ratios of P-to-R, which was pre-calcined at 500°C for 2h.

P/R Molar ratio	Surface Area (m ² /g)	Mass loss (%)
0.3	76.6	12
0.5	99.7	11.3
1	82	-2.07
1.5	140.4	12.6
Neat P	73.9	10.6
Neat R	146.8	8.66

* Source: PRED Materials international, Inc.

4.2 Effect of silica-to-carbon molar ratio

In this section, silica/PRF composites were prepared with various silica-to-carbon (SiO_2/C) molar ratios and were fixed the molar ratio of phenol-to-resorcinol (P/R), resorcinol-to-formaldehyde (R/F), resorcinol-to-water (R/W) at 0.3, 0.5, and 0.15, respectively and sodium carbonate-to-water (C/W) 10 mol/m^3 .

Figure 4.9 shows FT-IR spectra of silica/carbon composite prepared at various SiO_2/C molar ratios. The characteristic absorption bands at wavenumber of 696 and 1100 cm^{-1} , which are associating with symmetric bending and antisymmetric stretching vibration of Si–O–Si bonding [39], are shown in all three composites. The signals of Si–O–Si bonding confirm the presence of silica in all composites. It is also witnessed that the increase in SiO_2/C molar ratio results in the increase in the signals of Si–O–Si bonding.

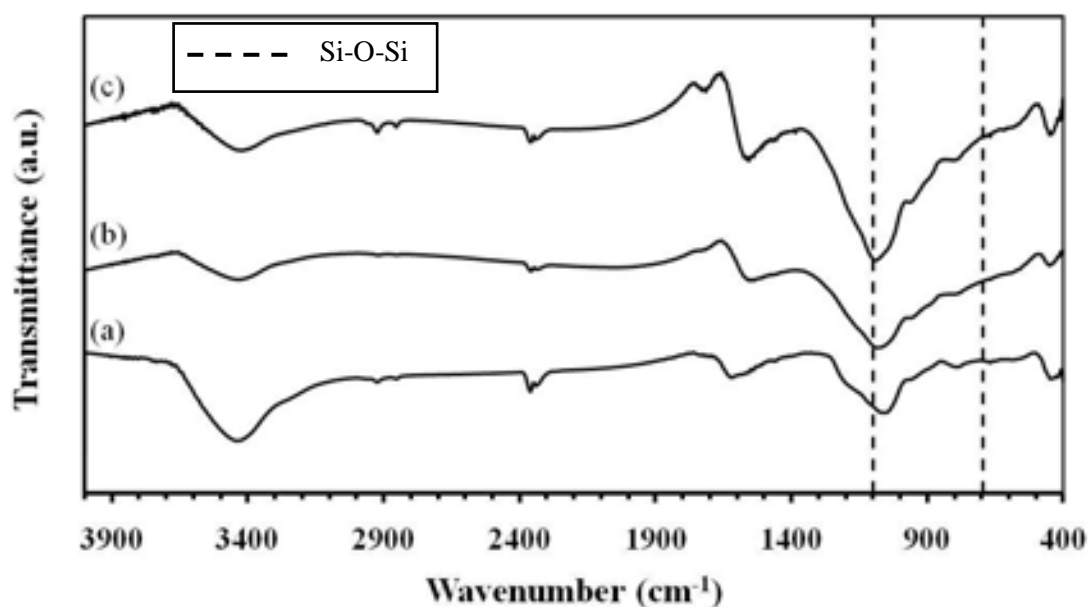


Figure 4.9 FTIR spectrum of silica/carbon composite prepared by using P/R molar ratio of 0.3 and various SiO_2/C molar ratios of 0.03 (a), 0.05 (b) and 0.07 (c).

The results from the XRD analysis of the final nitrided products prepared using various values of silica-to-carbon molar ratio are shown in Figure 4.10. It can be seen that the SiO_2/C molar ratio does not influence on the formation of silicon nitride but has an effect on the compositions of the products. At the molar ratio of SiO_2/C 0.03, it is found that the products obtained are crystalline silicon nitride, mainly in α -phase with small fraction of β -silicon carbide. Silicon carbide is formed by the manner as previously described. It may be caused by low SiO_2/C molar ratio. With the decreasing of SiO_2/C molar ratio, the amount of SiC increased sharply [44]. On the contrary, for the product, which prepared from the molar ratio of SiO_2/C 0.05 and 0.07, only α -phase of silicon nitride was detected. It is suggested that high molar ratio of SiO_2/C is suitable for silicon nitride synthesis, which has no by-product obtained. From the sharpness of the peaks detected, it is suggested that the product with molar ratio of 0.07 has higher crystallinity than the other two.

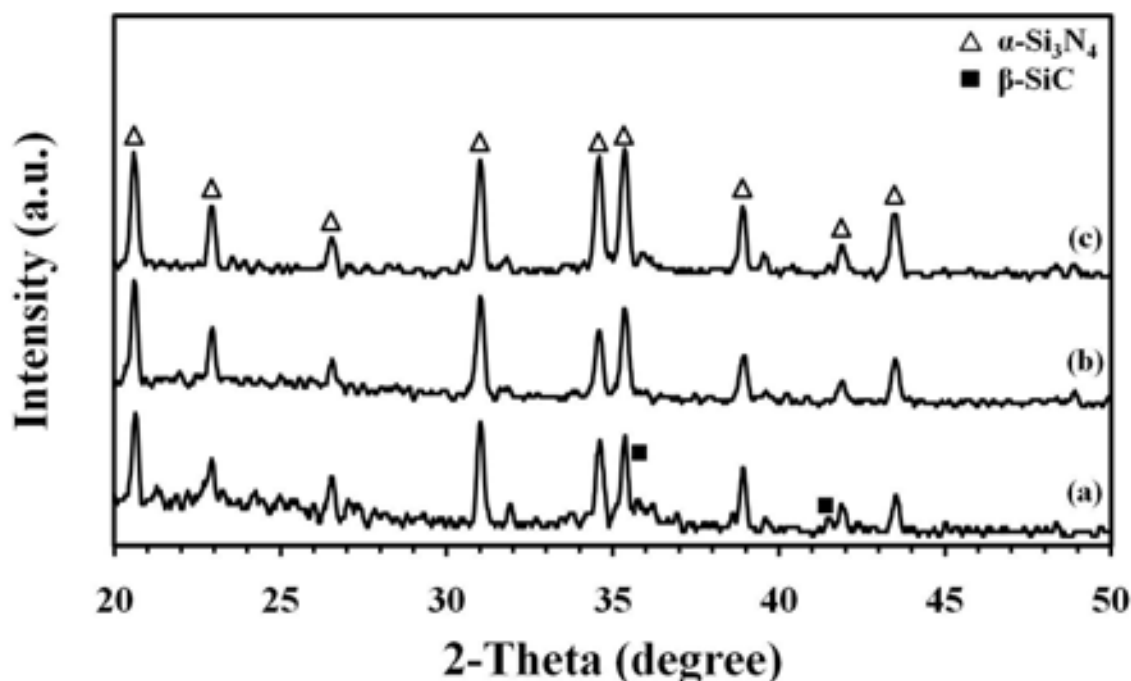


Figure 4.10 XRD patterns of silicon nitride powder, after the final calcination at 800°C for 8 h. The products were synthesized with SiO_2/C molar ratios of 0.03 (a), 0.05 (b), and 0.07 (c). The P/R molar ratio was fixed at 0.3.

The average crystallite sizes of the sample calculated from the Scherrer equation are shown in Table 4.6. It is found that the average crystallite size of the sample with SiO_2/C molar ratio of 0.03 is around 44 nm, which is larger than the other two samples. At the higher molar ratio of SiO_2/C (i.e., 0.05 and 0.07), the products have similar crystallite size was around 35 nm. It should also be noted that the grain size of the product, which was observed by scanning electron microscopy (Figure 4.11) is much larger than the calculated crystallite size. Therefore, the particles observed by SEM are in fact that a result of the agglomeration of the crystallites.

Table 4.6 Crystallite sizes of silicon nitride powder, after the final calcination at 800°C for 8 h. The products were synthesized from silica/PRF composites with various molar ratios of SiO_2/C .

SiO_2/C Molar ratio	Average crystallite size (nm)
0.03	44.1
0.05	35.3
0.07	35.1

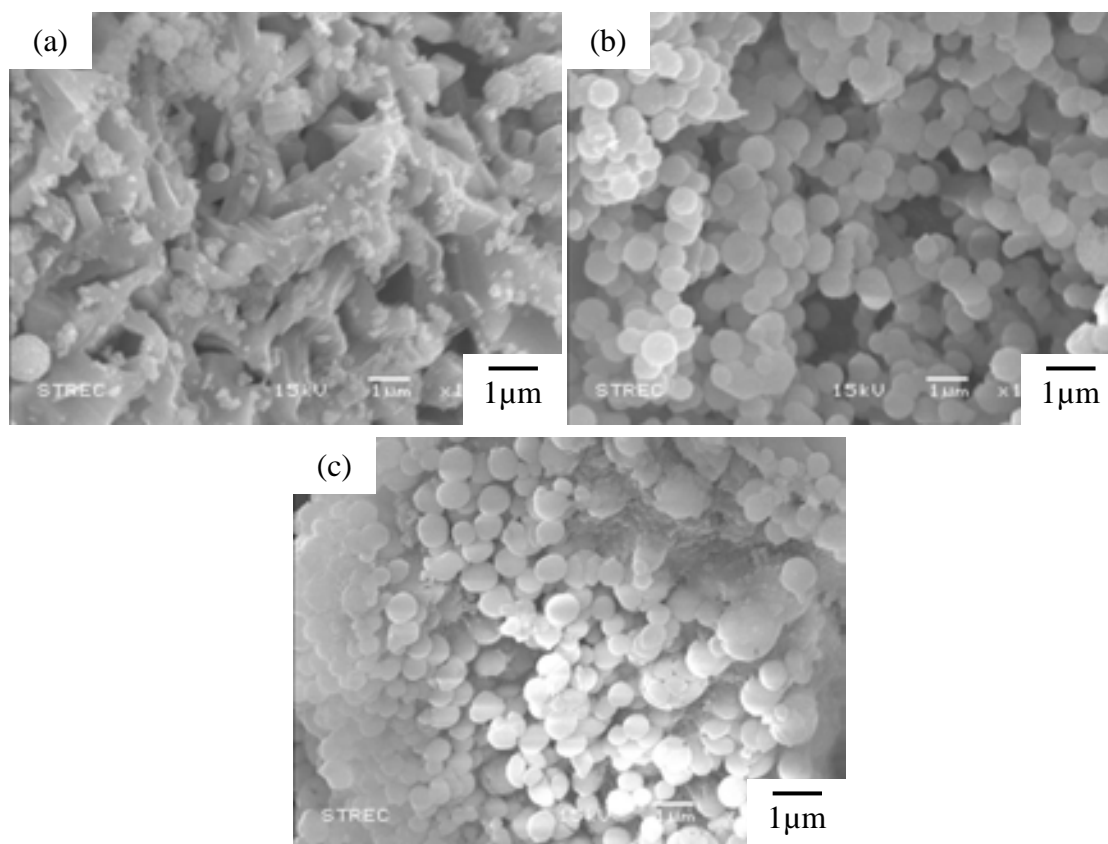


Figure 4.11 SEM micrographs of the silicon nitride products synthesized with various SiO_2/C molar ratios, after the final calcination: (a) 0.03; (b) 0.05 and (c) 0.07.

Table 4.7 summarizes the specific surface area of the samples after two preparation steps (i.e., before nitridation and after final calcination). It indicates that all products synthesized in this section are porous silicon nitride. The final products, prepared with SiO_2/C molar ratio of 0.03 and 0.05, retain high specific surface area comparing with the silica/carbon composites. The pyrolyzed composites with the high surface area also produce the final product with high surface area. It is suggested that the pyrolyzed composite, which has high specific surface area, allows N_2 and H_2 gas to easily diffuse into pores of the composite to react with silica and carbon to form silicon nitride product. On the contrary, the surface area of the final product prepared with SiO_2/C molar ratio of 0.07 is dramatically decreased comparing with its silica/carbon composite form. It should be noted that at the high SiO_2/C molar ratio

(0.07), the pore collapse during calcination process where carbon in the sample is burnt out and silica in the silica/carbon composite agglomerates, causing the decrease in surface area of the sample. In this section, the maximum surface area of the final product obtained is at SiO₂/C molar ratio of 0.05. Decreasing in surface area of the final product is a result of the removal of residual carbon in the calcination process.

From the TGA results (Table 4.8), it is confirmed that the residual carbon was mainly removed from the product. So, the surface area measured belongs to the Si₃N₄ and SiC products, not to the residual carbon.

Table 4.7 Surface areas of pyrolyzed silica/carbon composite and final products silicon nitride synthesized with various SiO₂/C molar ratios.

SiO ₂ /C Molar ratio	Surface area (m ² /g)	
	Silica/carbon composites (After 1 st calcination, 450°C for 2h)	Silicon nitride powders (After final calcination)
0.03	411.5	173.1
0.05	435.5	194.1
0.07	306.3	59.9

Table 4.8 Mass loss from TGA analysis of silicon nitride products after the final calcination. The analysis were done in oxygen atmosphere. The composites were prepared from silica/PRF gel with various molar ratios of SiO₂/C.

SiO ₂ /C Molar ratio	Mass loss (%)
0.03	12
0.05	11
0.07	8.1

The pore size distributions of the silica/carbon composite, prepared with various molar ratios of SiO_2/C after being calcined at 450°C for 2 h, are shown in Figure 4.12. The pore size distribution curves were obtained from N_2 adsorption isotherm using the Barret-Joyner-Halenda (BJH) method. No significant difference in average pore size between the three samples was observed. All silica/carbon composites, which are consisting mainly of carbon, exhibit narrow pore size distribution around 3.3 nm. Figure 4.13 shows pore size distributions of the final products, after removing the residual carbon. After the final calcination step, the samples have different pore size distribution, although all of the final products are still mesoporous silicon nitride. The sample with SiO_2/C molar ratio of 0.03 exhibits bimodal pore size distribution at around 4.2 and 14 nm, respectively, while the sample with SiO_2/C molar ratio of 0.05 shows narrow pore size distribution at around 4 nm. The sample with the highest SiO_2/C molar ratio appears with wide range of pore size distribution from 5.4 to 16 nm. Pore size of the product becomes larger as a result of the N_2 diffused into the pore of silica/carbon composite to react with SiO_2 and carbon to form the final products.

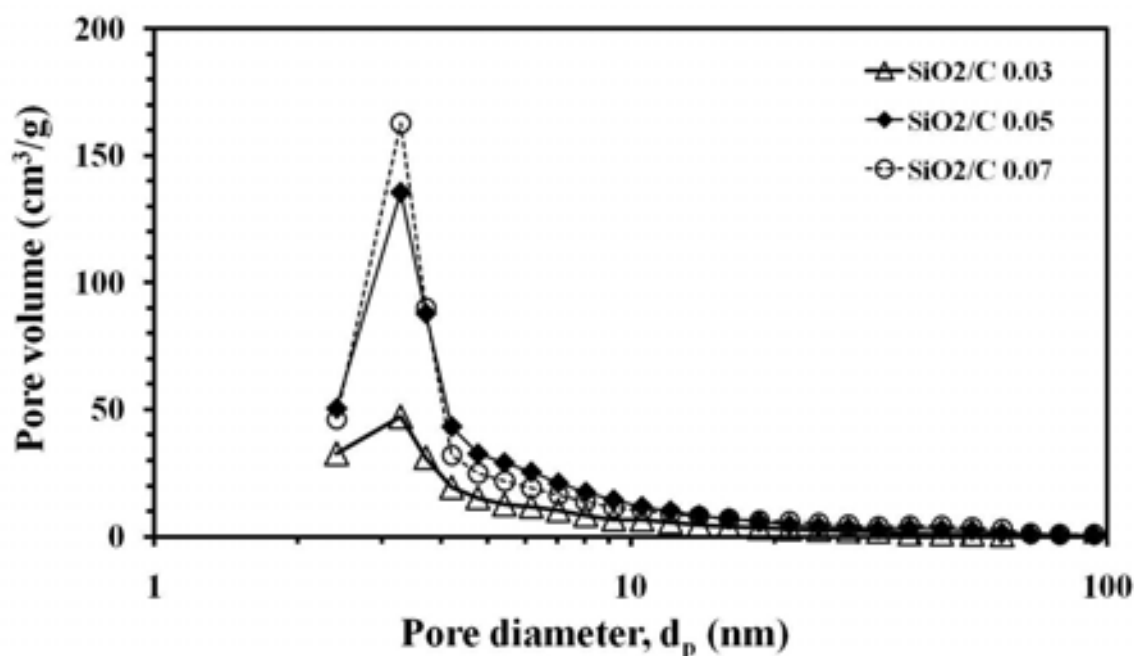


Figure 4.12 Pore size distribution of pyrolyzed silica/PRF composites after being calcined at 450°C for 2 h. The samples were prepared by pyrolysis of silica/PRF gels synthesized with various molar ratios of SiO_2/C .

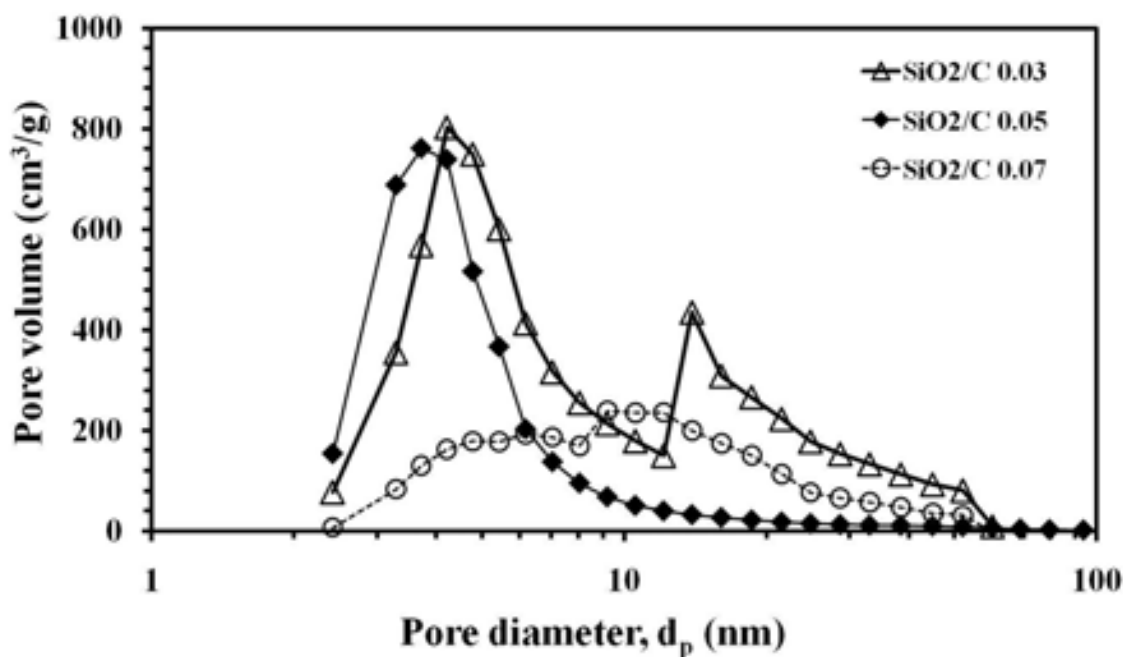


Figure 4.13 Pore size distribution of silicon nitride product, after the final calcination at 800°C for 8 h. The products were prepared by pyrolysis of silica/PRF gels synthesized with various molar ratios of SiO₂/C.

Although all of the samples are mesoporous silicon nitride, the difference in shape of hysteresis loop in the adsorption isotherm indicates that pore structures of the samples are different. According to Figure 4.14, one can see that all of the samples show type IV isotherms with strong affinities. The product with SiO₂/C molar ratio of 0.03 has hysteresis loop of H-3 type, which is believed that this type of isotherm occurs with aggregates of particles giving rise to slit-shaped pores [45]. The other two products, which have higher SiO₂/C molar ratio, reveal hysteresis loop of H-4 type, which is associated with narrow slit-like pores [45]. The type IV adsorption isotherm is typical for mesoporous materials. It is suitable for gas filter application, which is used to separate micron-sized solid particles such as dust from gas stream.

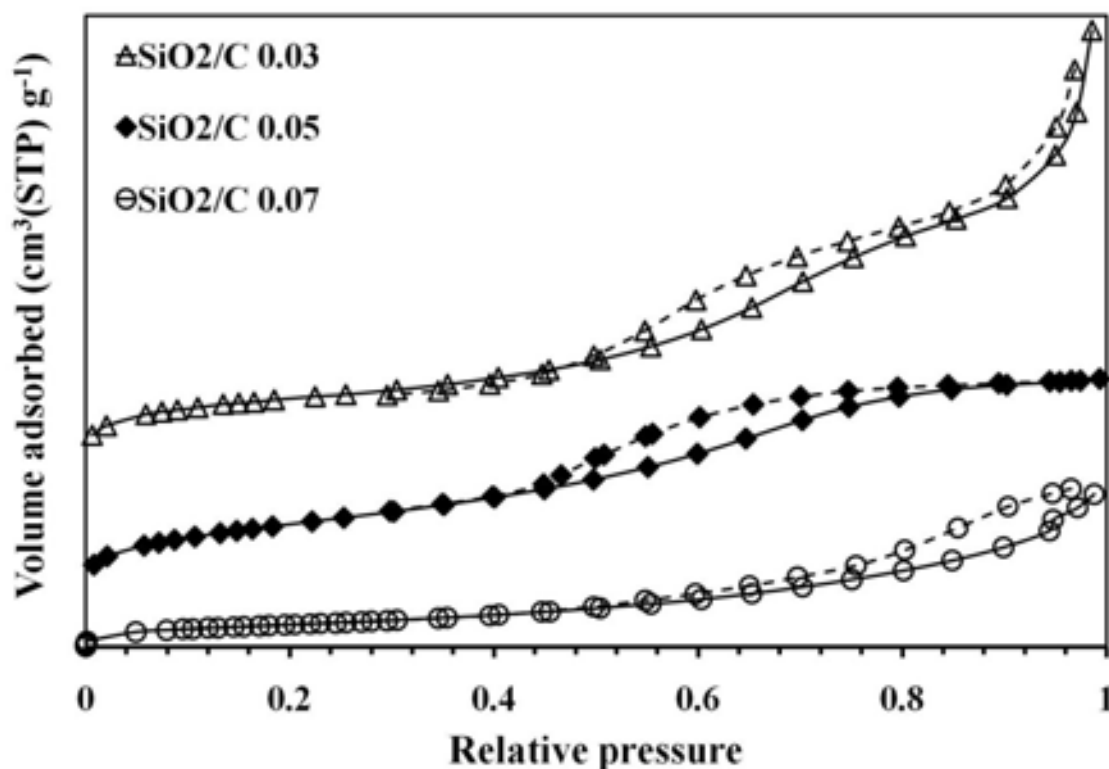


Figure 4.14 Adsorption (—) and desorption (---) isotherms of N_2 on silicon nitride products, after the final calcination at 800°C for 8 h. The products were prepared by pyrolysis of silica/PRF gels synthesized with various molar ratios of SiO_2/C .

4.3 Effect of the calcination of the pyrolyzed composite

In this part, effect of the controlled calcination of the silica/carbon composite to partially remove carbon to enhance porosity of the composite is investigated. The silica/carbon composites used in this part were prepared with P/R and Si/C molar ratios of 0.3 and 0.03, respectively.

The specific surface areas and TGA results of the samples after two preparation steps (i.e., before nitridation and after final calcination) are shown in Table 4.9. The surface area of the pyrolyzed silica/carbon composite is increased when the calcination temperature is increased, corresponding the content of remaining

carbon in the composites measured by TGA. It is suggested that the enhanced surface area is a result from the loss of carbon derived from part of the PRF-gel in the composite. It is found that the surface area of silica/carbon composite is generally increased after being pre-calcined. During the pre-calcination process, only carbon reacts with oxygen in air, which was partially burnt out from the composite, not silica. Silica is stable in the range of pre-calcined temperature (400-500°C) and does not react with air in the process. Both of surface area of the final products, which pre-calcined at 500 and 450°C, are dramatically decreased comparing to that of silica/carbon composites because the final products have lower carbon content than that of silica/carbon composites. On the other hand, the composite was pre-calcined at 400°C, produces the final product with increased surface area, although its initial surface area before the nitridation process was low. The results in this condition cannot be explained.

Table 4.9 Specific surface area and carbon content of silica/carbon composite after being calcined and that of the final nitrated product, as a function of the calcination temperature of the silica/carbon composite.

Temperature for calcination of the silica/carbon composite (°C)	Silica/carbon composite after calcination		Final product after final calcination	
	Surface area (m ² /g)	Carbon content (%)	Surface area (m ² /g)	Carbon content (%)
400	5.71	70.2	189.6	5.58
450	411.5	56.8	173.1	11.1
500	453.3	37.5	53.2	8.70

Pore size distribution of silica/carbon composites after calcination and silicon nitride products after the final calcination are shown in Figure 4.15 and 4.16, respectively. For the samples firstly calcined at 400°C, the pore size distribution of the silicon nitride products is similar to that of its silica/carbon composites. Both of

distribution curves have a single peak and the value for pore diameter of the maximum is at 4.7 nm. For the sample firstly calcined at 450°C, its silica/carbon composite has a narrow pore size distribution, of which the maximum is located at 3.3 nm. The final product, which was subjected to nitridation process and subsequently calcined at 800°C, exhibits bimodal pore distribution. The first peak is located at about 4.2 nm while the second peak is at about 14 nm. This indicates that the larger pore in the final nitride product obtained from the final calcination process where residual carbon was burnt out, congruent with the lower in surface area. For the sample firstly calcined at 500°C, silicon nitride product shows a narrow pore size distribution with pore diameter of 3.3 nm, although its silica/carbon composite has the pore size ranging in both mesopore and micropore (as shown in inset).

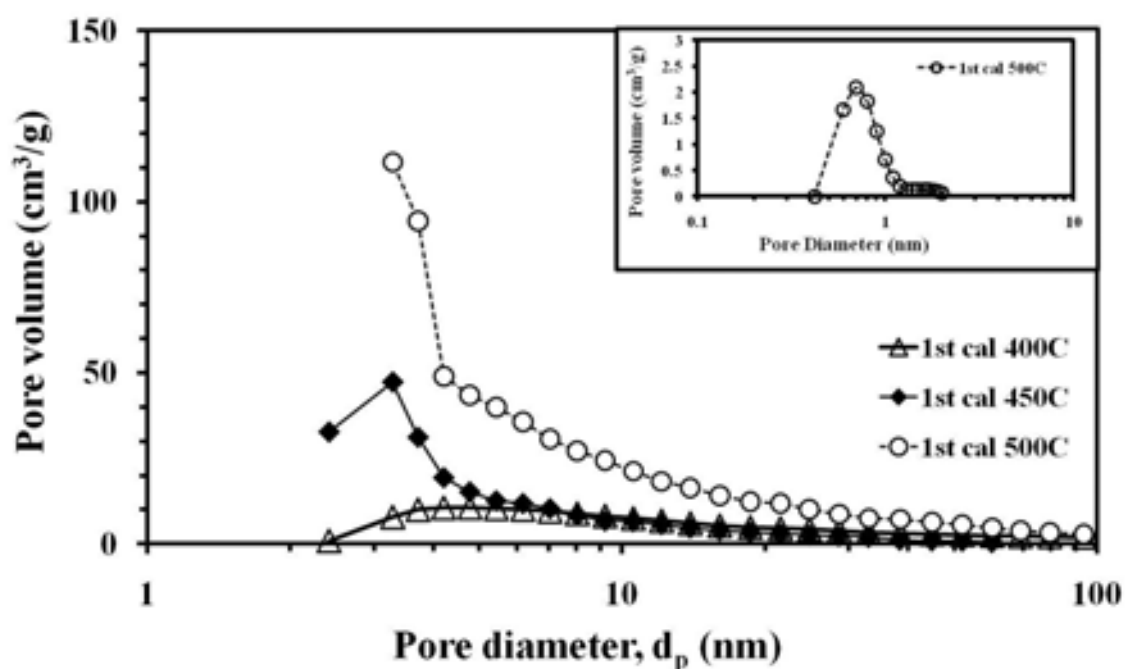


Figure 4.15 Pore size distributions of the silica/carbon composites after the 1st calcination at various temperatures. The samples were prepared from silica/PRF composite synthesized with P/R and SiO₂/C ratio of 0.3 and 0.03, respectively.

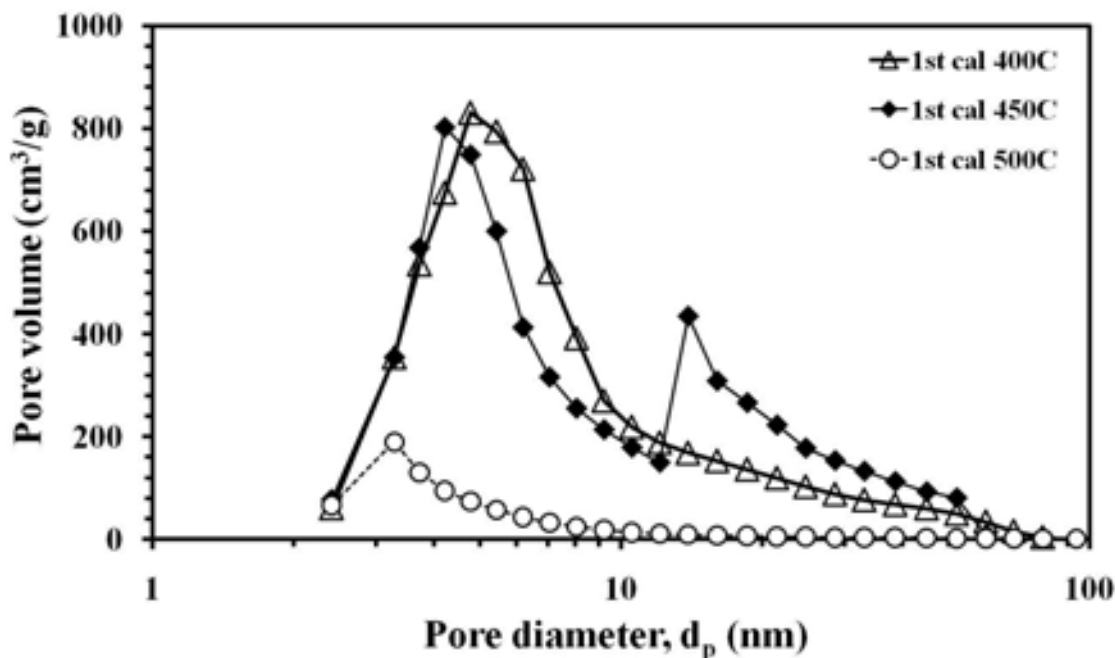


Figure 4.16 Pore size distributions of the final products after the 2nd calcination. The samples were prepared from silica/PRF composite synthesized with P/R and SiO₂/C ratio of 0.3 and 0.03, respectively and subjected to the 1st calcination at various temperatures.

The X-ray diffraction analysis results of the products from the nitridation are shown in Figure 4.17. According to the XRD analysis, all of the nitrated products after the final calcination are mainly α -silicon nitride. Only α -silicon nitride was detected in the product that was pre-calcined at 500°C, while both α -silicon nitride and β -silicon carbide appeared in products, which were pre-calcined at 400 and 450°C. According to the TGA results (Table 4.9), the silica/carbon composite calcined at 500°C has lower carbon content (37.5 wt% carbon), than the composites calcined at lower temperature. It should be noted that the low carbon content in the composite can prevent the formation of silicon carbide. Nevertheless, it can be seen that the calcination of the silica/carbon composite to partially remove carbon and enhance porosity of the composite does not affect the formation of silicon nitride.

The crystallite sizes of silicon nitride products were calculated from the Scherrer equation. It is found that the crystallite size increased with an increase in calcination temperature, as shown in Table 4.10.

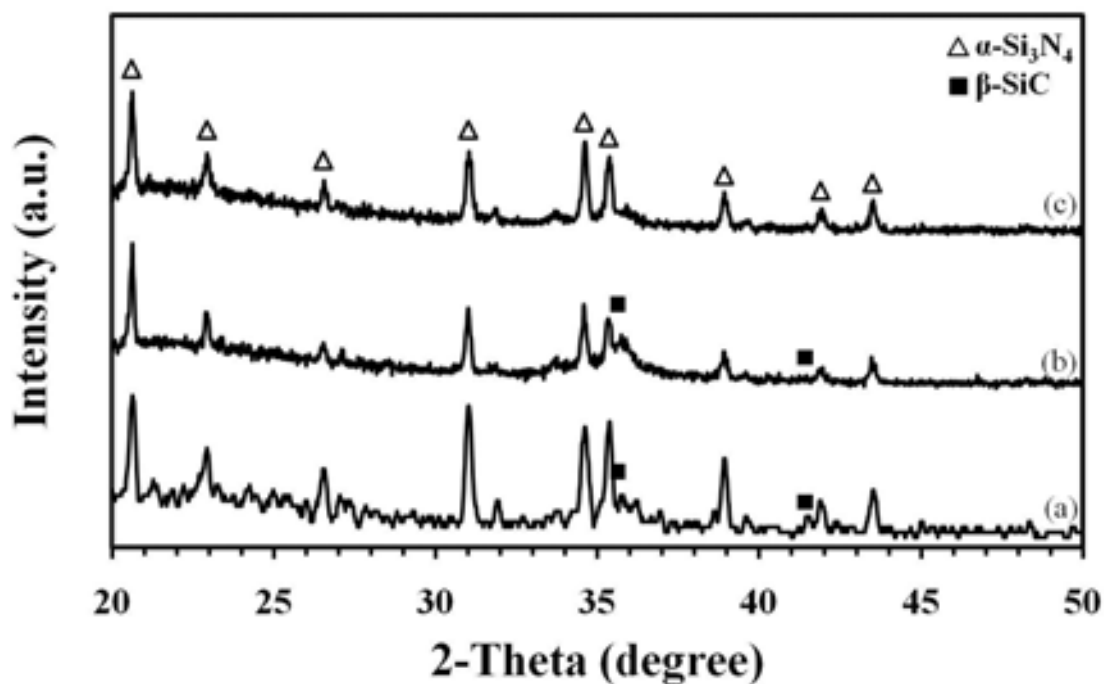


Figure 4.17 XRD patterns of silicon nitride powder, after the final calcination at 800°C for 8 h. The products were prepared from silica/PRF composite with P/R and SiO_2/C ratio 0.3 and 0.03. The silica/carbon composites were calcined at various calcination temperatures: (a) 400°C, (b) 450°C and (c) 500°C before nitridation.

Table 4.10 Crystallite sizes of silicon nitride powder, after calcination at 800°C for 8 h. The products were prepared from silica/PRF composite with P/R and Si/C ratio 0.3 and 0.03. The silica/carbon composites were calcined at various calcination temperatures: (a) 400°C, (b) 450°C and (c) 500°C before nitridation.

Temperature for calcination of the silica/carbon composite (°C)	Average crystallite size (nm)
400	44.2
450	52.5
500	106.6

4.4 The use of silica sol as silica source

In this section, silica precursor was firstly prepared to form silica sol by mixing with water and ethanol before being added into PRF solution. This is another way to decrease violent interaction between silica precursor and the PRF gel.

According to Figure 4.18, XRD patterns in both samples contained α -silicon nitride, β -silicon nitride and β -silicon carbide. However, the crystallinity of the two products is different. The product, which was prepared from pre-formed silica sol has greater crystallinity than the other one. It can be seen from sharper peaks and higher in intensity. It should be note that the use of pre-formed sol has no effect on the formation of silicon nitride but has an effect on crystallinity of the product. The average crystallite size of the product synthesized from the pre-formed sol is larger than product, which was prepared by normally prepared silica/carbon composite, as shown in Table 4.11. The results are congruent with SEM micrograph, in which the pre-formed sol product shows larger grain (Figure 4.19).

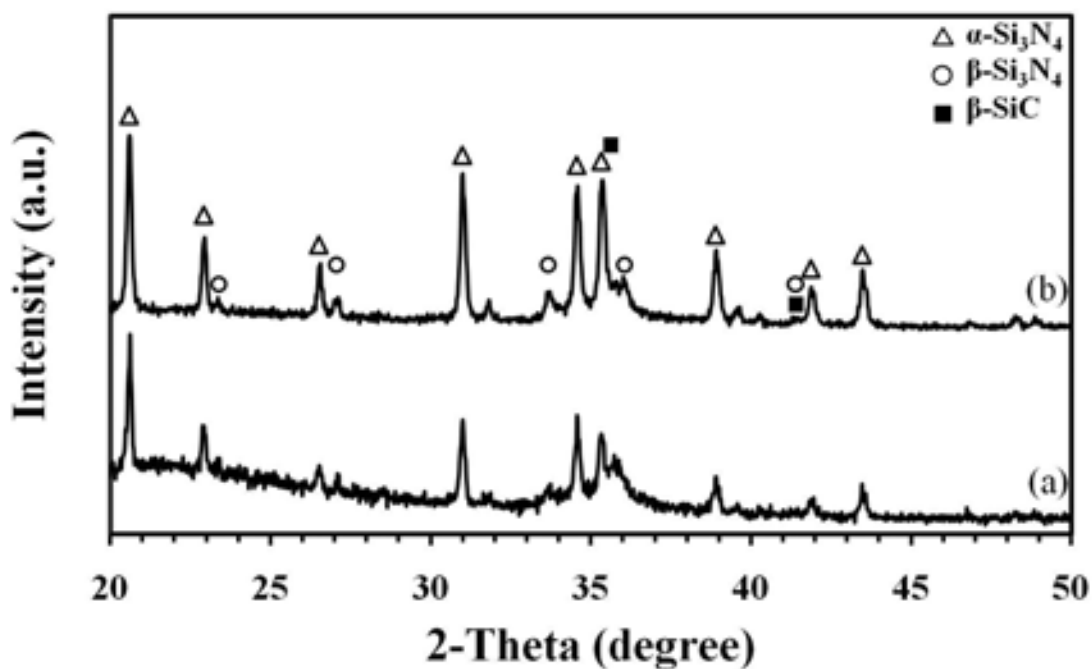


Figure 4.18 XRD patterns of silicon nitride powder, after the final calcination at 800°C for 8 h. The products were prepared from synthesized using APTMS (a) and pre-formed silica sol (b) as the silica source. The P/R and SiO_2/C molar ratio were fixed at 0.3 and 0.03, respectively.

Table 4.11 Crystallite sizes of silicon nitride powder, after calcination at 800°C for 8 h. The products were prepared from synthesized using APTMS and pre-formed silica sol as the silica source. The P/R and SiO_2/C molar ratio were fixed at 0.3 and 0.03, respectively.

Source of silica	Average crystallite size (nm)
APTMS	40.0
silica sol	60.3

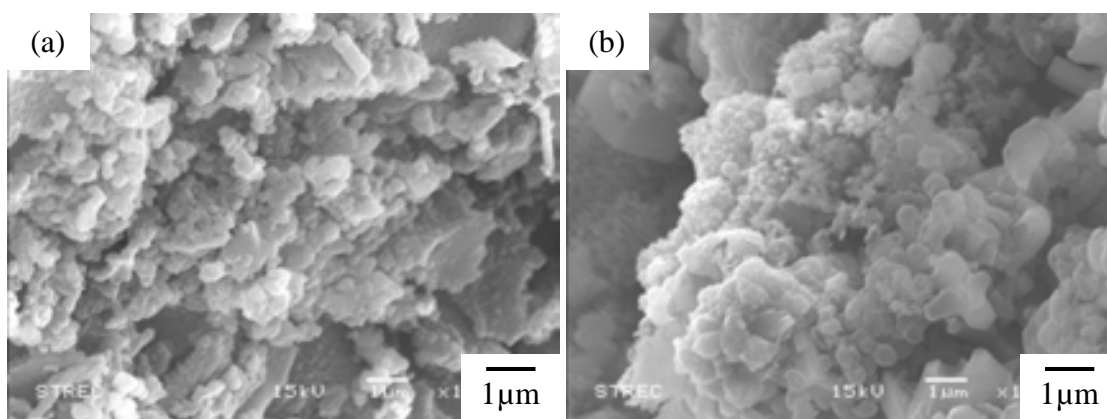


Figure 4.19 SEM micrographs of the silicon nitride products after final calcination.

The products were prepared from synthesized using APTMS (a) and pre-formed silica sol (b) as the silica source. The P/R and SiO_2/C molar ratio were fixed at 0.3 and 0.03, respectively.

The specific surface area and the pore size distribution calculated from BJH model are reported in Table 4.12 and Figure 4.20 - 4.21, respectively. For the pyrolyzed composites, it is shown that although both pyrolyzed composites have high surface area, the composite prepared using pre-formed silica sol has quite higher surface area. It is conform to the TGA results that the content of carbon remaining in the composites is inversely related to the specific surface area. It shows that the enhanced surface area is a result from the loss of carbon derived from part of the PRF-gel in the composites as previously mentioned. Figure 4.20 reveals pore size distribution of both pyrolyzed composites. It appears as bimodal pore size distribution for the composite derived from pre-formed silica sol with one peak located around 3.7 nm and the other is around 16 nm. On the other hand it appears as narrow pore size distribution at 3.3 nm for the pyrolyzed silica/carbon composite prepared using APTMS as silica source.

Table 4.12 Specific surface areas and carbon content of pyrolyzed silica/carbon composite and the final nitride products after calcination at 800°C for 8 h. The products were prepared from synthesized using APTMS and pre-formed silica sol as the silica source. The P/R and SiO₂/C molar ratio were fixed at 0.3 and 0.03, respectively.

Source of silica	Pyrolyzed composites (After 1 st calcination, 450°C for 2h)		Silicon nitride powders (After final calcination)	
	Surface area	Carbon	Surface area	Carbon
	(m ² /g)	content (%)	(m ² /g)	content (%)
APTMS	411.5	70	173.1	11.0
silica sol	487	50	40.7	2.26

For the final nitride products, both of the products after the final calcination have much lower surface area than that of the pyrolyzed composites. It suggests that the pyrolyzed composites contained a lot of carbon content. So, after the final calcination, carbon was burnt out and leaving with lower surface area. According to Figure 4.21, shows the pore size distribution of the final product, synthesized from using APTMS compared with pre-formed silica sol as the silica source. The final product synthesized using APTMS exhibits bimodal pore distribution at 4.2 and 13.9 nm, respectively, which suggests that products are not uniform. It should be noted that the amount of residual carbon in the final product prepared from normal silica/carbon composite is found to be 11 %. Hence, the small pores observed might belong to residual carbon in the product, while the larger pores are belonging to silicon nitride product. On the other hand, the final product, synthesized using pre-formed silica sol reveals a narrow pore size distribution with the average pore size of around 13.9 nm. According to the TGA results, it has only 2.26% carbon content left in the product. Therefore, the surface area and pore diameter measured belongs to the Si₃N₄ products, not to the residual carbon.

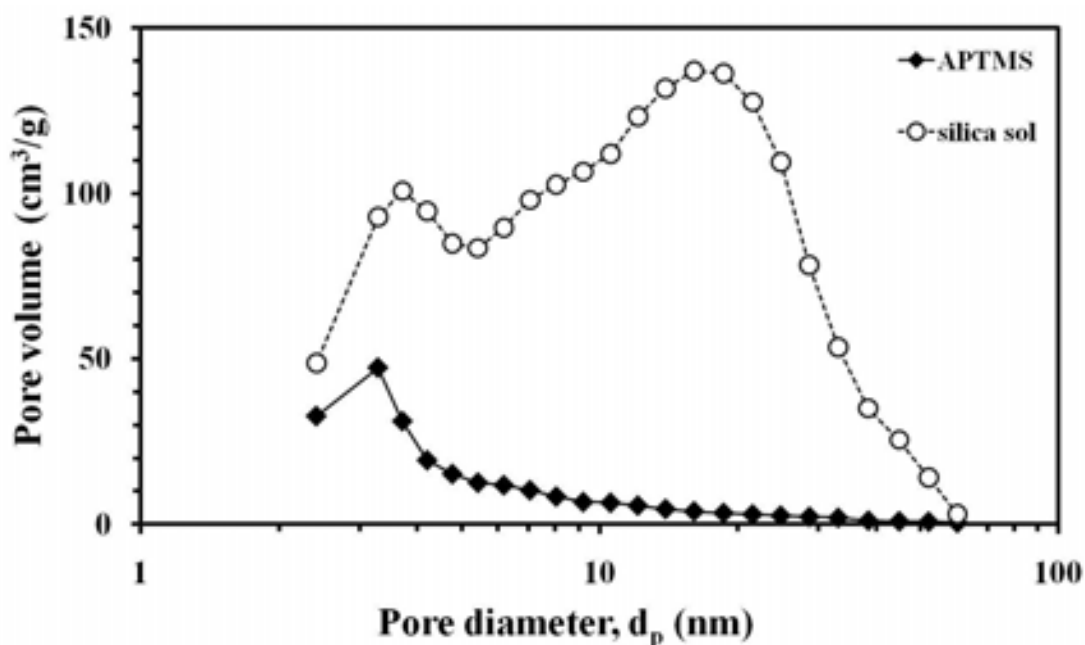


Figure 4.20 Pore size distributions of the silica/carbon composites after 1st calcination. The composites were prepared from synthesized using APTMS and pre-formed silica sol as the silica source. The P/R and SiO₂/C molar ratio were fixed at 0.3 and 0.03, respectively.

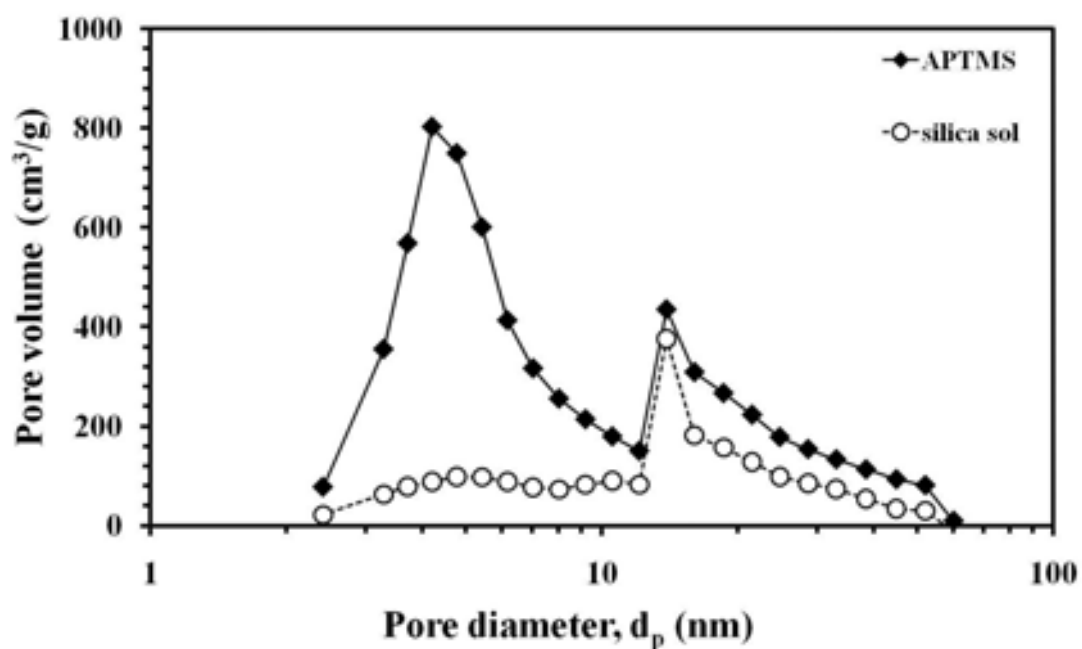


Figure 4.21 Pore size distributions of the silicon nitride products after final calcination. The products were prepared from synthesized using APTMS and pre-formed silica sol as the silica source. The P/R and SiO₂/C molar ratio were fixed at 0.3 and 0.03, respectively.

Representative N_2 adsorption–desorption isotherms of the silicon nitride products, which was synthesized using different kind of silica source are shown in Figure 4.22. Both products give mesoporous structure and display a typical type IV isotherm (according to IUPAC) [46]. The product prepared using APTMS as the silica source has hysteresis loop type H-3 in the isotherms may indicate the presence of slit-shaped pores [45] in the silicon nitride product. While the product derived from pre-formed silica sol shows hysteresis loop similar the loop of type H-4, which often is associated with narrow slit-like pores [45].

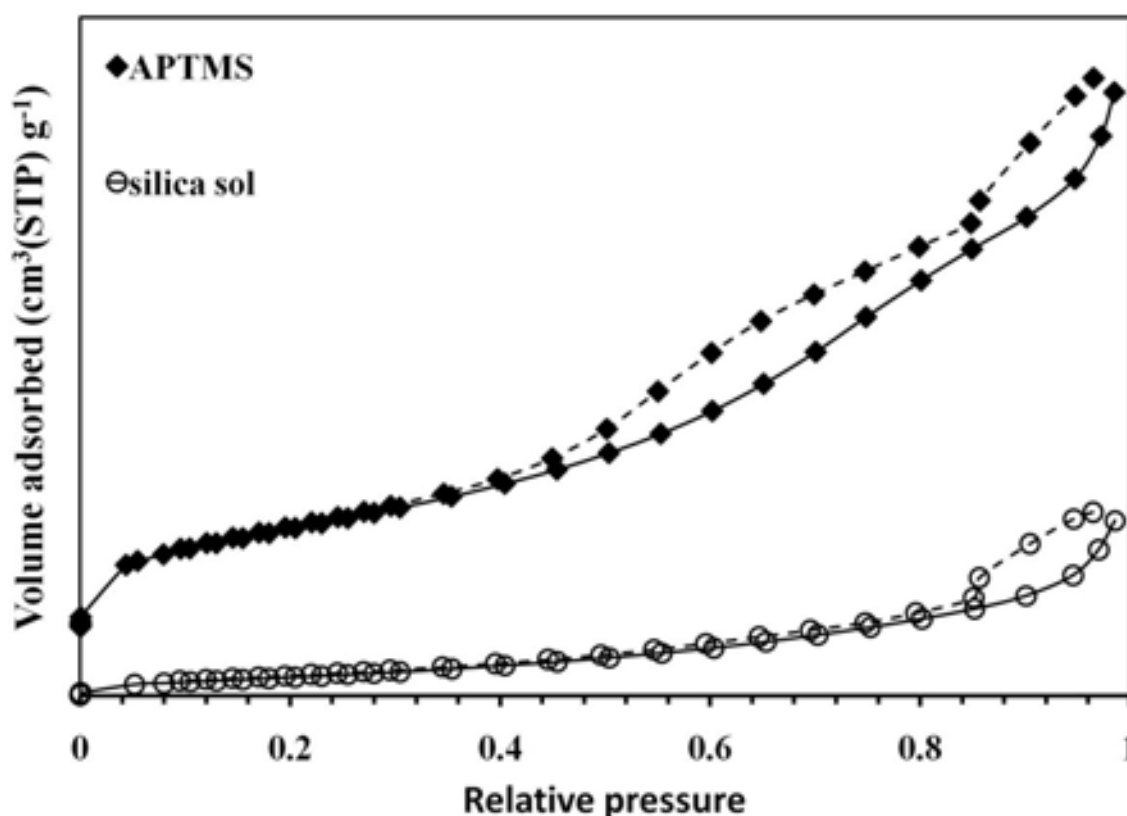


Figure 4.22 Adsorption (—) and desorption (---) isotherms of N_2 on silicon nitride products, after calcination at 800°C for 8 h. The products were prepared from synthesized using APTMS and pre-formed silica sol as the silica source. The P/R and SiO_2/C molar ratio were fixed at 0.3 and 0.03, respectively.

CHAPTER V

CONCLUSIONS AND RECOMMENDATIONS

5.1 Summary of the results

1. Porous silicon nitride can be fabricated from silica/PRF gel composite via the carbothermal reduction and nitridation. Although most products synthesized in this work are mainly crystalline α -silicon nitride, some products produced are mixed with β -phase of silicon carbide.
2. Composition of two types of carbon precursors (i.e., resorcinol and phenol) has influence on surface area of pyrolyzed silica/PRF composite and the uniformity of particles.
3. Molar ratio of silica and carbon has influence on surface area of silicon nitride product. In this work, lower SiO_2/C molar ratio (0.03 and 0.05) gives higher surface area in both pyrolyzed composites and silicon nitride products.
4. The pre-calcination of the silica/carbon composite at lower temperature (400-500°C) is an alternative way to enhance porosity of the composite before subjected to nitridation process. The surface area of the pyrolyzed silica/carbon composite is increased when the calcination temperature is increased, which is a result from the loss of carbon derived from part of the PRF-gel in the composites.
5. The use of pre-formed silica sol is another way to decrease violent interaction between silica precursor and the PRF solution. The result shows that, the product, which was prepared by pre-formed sol presents

small average crystallite size. Although the pyrolyzed pre-formed sol silica/carbon composite gives higher surface area, the surface area of the product is lower than the product synthesized using APTMS as silica source.

5.2 Conclusions

Porous silicon nitride can be fabricated from silica/PRF gel composite via the carbothermal reduction and nitridation. All of the investigated effects (i.e., composition of the phenol-resorcinol-formaldehyde gel, silica-to-carbon molar ratio of the composites, calcination temperature and the use of pre-formed silica sol enhance the porosity of silica/carbon composite in difference. The pre-calcination is the major effect to improve the porosity, which has an effect on porosity of silicon nitride product. Effect of the composition of phenol-resorcinol-formaldehyde gel and the silica-to-carbon molar ratio have influence on porosity of the product, although quite difference on porosity of composite. The use of pre-formed silica sol is an alternative route to avoid violent interaction between silica precursor and the PRF solution, which affects different in crystallite size of the product. All of most products synthesized in this work are mainly in crystalline α -silicon nitride, some products produced are mixed with β -phase of silicon carbide. Moreover, the silicon nitride products synthesized in this work have much higher surface area than the conventional silicon nitride granules, which indicates significant increase in porosity.

5.3 Recommendations for Future Work

Synthesis of porous silicon nitride from silica/PRF gel composite via the carbothermal reduction and nitridation process as well as effects of various factors, such as composition of the PRF-gel, silica-to-carbon molar ratio of the composite, pre-calcination of silica/carbon composite, and the use of pre-formed silica sol as

silica source have been investigated in this work. Some recommendations for future work are listed as follows:

1. Thermodynamic calculation of the carbothermal reduction and nitridation process should be investigated in detail.
2. The applications of silicon nitride powders should be further investigated.

REFERENCES

- [1] Koc, R., and Kaza, S. Synthesis of α -Si₃N₄ from carbon coated silica by carbothermal reduction and nitridation. Journal of the European Ceramic Society 18 (1998): 1471-1477.
- [2] Turkdogan, E.T., Bills, P.M., and Tippet, V.A. Silicon nitrides: Some physico-chemical properties. Journal of Applied Chemistry 8 (1958): 296-302.
- [3] Lange, F.F. Fracture toughness of silicon nitride as a function of the initial α -phase content. Journal of American Ceramic Society 62 (1979): 428-430.
- [4] Ziegler, G., Heinrich, J., and Wötting, G. Relationships between processing, microstructure and properties of dense and reaction-bonded silicon nitride. Journal of Materials Science 22 (1987): 3041-3086.
- [5] Yang, J.-F., Ohji, T., Zeng, Y.-P., Kanzaki, S., and Zhang, G.-J. Fabrication and mechanical properties of porous silicon nitride ceramics from low-purity powder. Ceramics Society of Japan 111 (2003): 758-761.
- [6] Díaz, A., and Hampshire, S. Characterisation of porous silicon nitride materials produced with starch. Journal of the European Ceramic Society 24 (2004): 413-419.
- [7] Yang, J.-F., Ohji, T., Kanzaki, S., Díaz, A., and Hampshire, S. Microstructure and Mechanical Properties of Silicon Nitride Ceramics with Controlled Porosity. Journal of the American Ceramic Society 85 (2002): 1512-1516.
- [8] Kawai, C., and Yamakawa, A. Effect of Porosity and Microstructure on the Strength of Si₃N₄: Designed Microstructure for High Strength, High Thermal Shock Resistance, and Facile Machining. Journal of the American Ceramic Society 80 (1997): 2705-2708.
- [9] Yang, J.-F., Deng, Z.-Y., and Ohji, T. Fabrication and characterisation of porous silicon nitride ceramics using Yb₂O₃ as sintering additive. Journal of the European Ceramic Society 23 (2003): 371-378.

- [10] Yang, J.-F., and Ohji, G.-J.Z.T. Porosity and microstructure control of porous ceramics by partial hot pressing Journal of Materials Research Society Symposium Proceedings 16 (2001): 1916-1918.
- [11] Fukasawa, T., Deng, Z.-Y., Ando, M., Ohji, T., and Kanzaki, S. Synthesis of Porous Silicon Nitride with Unidirectionally Aligned Channels Using Freeze-Drying Process. Journal of the American Ceramic Society 85 (2002): 2151-2155.
- [12] Pekela, R.W. Organic Aerogels from the Polycondensation of Resorcinol with Formaldehyde. Journal of Materials Science 24 (1989): 3221-3227.
- [13] Pekala, R.W., Alviso, C.T., Lu, X., Groß, J., and Fricke, J. Journal of Non-Crystalline Solids 188 (1995)
- [14] Freitag., D.W., and Richardson., D.W. Ceramic Industry. Advancing Advanced Ceramics and Glasses: 1-6.
- [15] Matovic, B. Low Temperature Sintering Additives for Silicon Nitride. Max-Planck-Institut für Metallforschung Stuttgart (2003): 1-133.
- [16] Zerr, A., et al. Synthesis of cubic silicon nitride. Nature 400 (1999): 340-342.
- [17] Hampshire, S. Silicon nitride ceramics – review of structure, processing and properties. Journal of Achievements in Materials and Manufacturing Engineering 24 (2007)
- [18] Yang, J.-F., et al. Synthesis of fibrous β - Si_3N_4 structured porous ceramics using carbothermal nitridation of silica. Acta Materialia 53 (2005): 2981-2990.
- [19] Arik, H. Synthesis of Si_3N_4 by the carbothermal reduction and nitridation of diatomite. Journal of the European Ceramic Society 23 (2003): 2005-2014.
- [20] Karakus, N., Kurt, A.O., and Toplan, H.Ö. Synthesizing high α -phase Si_3N_4 powders containing sintering additives. Ceramics International 35 (2009): 2381-2385.
- [21] Jia, L., Y.Zhang, and Gu, J.-H. Preparation of porous Si_3N_4 ceramics with β - Si_3N_4 as seeds. Journal of Synthetic Crystals 37 (2008): 1224-1227.

- [22] Li, J., and Riedel, R. Carbothermal Reaction of Silica–Phenol Resin Hybrid Gels to Produce Silicon Nitride/Silicon Carbide Nanocomposite Powders. Journal of the American Ceramic Society 90 (2007): 3786-3792.
- [23] Al-Muhtaseb, S.A., and Ritter, J.A. Properties of Resorcinol-Formaldehyde Organic and Carbon Gels. Journal of Advanced Materials 15 (2003)
- [24] Pekala, R.W. Organic aerogels from the polycondensation of resorcinol with formaldehyde. Journal of Materials Science 24 (1989): 3221-3227.
- [25] Tamon, H., Ishizaka, H., Yamamoto, T., and Suzuki, T. Preparation of mesoporous carbon by freeze drying. Carbon 37 (1999): 2049-2055.
- [26] Ruben, G.C., Pekala, R.W., Tillotson, T.M., and Hrubesh, L.W. Imaging aerogels at the molecular level. Journal of Materials Science 27 (1992): 4341-4349.
- [27] Yamamoto, T., Mukai, S.R., Endo, A., Nakaiwa, M., and Tamon, H. Interpretation of structure formation during the sol-gel transition of a resorcinol-formaldehyde solution by population balance. Journal of Colloid and Interface Science 264 (2003): 532-537.
- [28] Lin, C., and Ritter, J.A. Effect of synthesis pH on the structure of carbon xerogels. Carbon 35 (1997): 1271-1278.
- [29] Czakkel, O., Marthi, K., Geissler, E., and László, K. Influence of drying on the morphology of resorcinol-formaldehyde-based carbon gels. Microporous and Mesoporous Materials 86 (2005): 124-133.
- [30] Schaefer, D.W., Pekala, R., and Beaucage, G. Origin of porosity in resorcinol-formaldehyde aerogels. Journal of Non-Crystalline Solids 186 (1995): 159-167.
- [31] Luyjew, K., Tonanon, N., and Pavarajarn, V. Mesoporous Silicon Nitride Synthesis Via the Carbothermal Reduction and Nitridation of Carbonized Silica/RF Gel Composite. Journal of the American Ceramic Society 91 (2008): 1365-1368.
- [32] Falbe, J., and Regitz, M. Roempp Chemie Lexikon, Thieme, Stuttgart (1992)
- [33] Gardziella, A., Pilato, L.A., and Knop, A. Phenolic Resins. Springer, Berlin (2000)

- [34] Mark, H.F., et al. Encyclopedia of Polymer Science and Technology, Wiley, New York 11 (1986): 49.
- [35] Knop, A., and Pilato, L.A. Phenolic Resins. Chemistry, Applications and Performance, Future Directions, Springer, Berlin (1985): 1.
- [36] Papadopoulou, E., and Chrissafis, K. Thermal study of phenol-formaldehyde resin modified with cashew nut shell liquid. Thermochimica Acta 512 (2011): 105-109.
- [37] Mukai, S.R., Tamitsuji, C., Nishihara, H., and Tamon, H. Preparation of mesoporous carbon gels from an inexpensive combination of phenol and formaldehyde. Carbon 43 (2005): 2628-2630.
- [38] Wu, D., Fu, R., Sun, Z., and Yu, Z. Low-density organic and carbon aerogels from the sol-gel polymerization of phenol with formaldehyde. Journal of Non-Crystalline Solids 351 (2005): 915-921.
- [39] Tian, R., et al. Infrared Characterization of Interfacial Si-O Bond Formation on Silanized Flat SiO₂/Si Surfaces. Langmuir 26 (2010): 4563-4566.
- [40] Al-Oweini, R., and El-Rassy, H. Synthesis and characterization by FTIR spectroscopy of silica aerogels prepared using several Si(OR)₄ and R''Si(OR')₃ precursors. Journal of Molecular Structure 919 (2009): 140-145.
- [41] Krajnc, I.P.a.M. Characterization of Phenol-Formaldehyde Prepolymer Resins by In Line FT-IR Spectroscopy. Acta Chimica Slovenica 52 (2005): 238-244.
- [42] Li, J., Wang, X., Huang, Q., Gamboa, S., and Sebastian, P.J. Studies on preparation and performances of carbon aerogel electrodes for the application of supercapacitor. Journal of Power Sources 158 (2006): 784-788.
- [43] Jin, G.-Q., and Guo, X.-Y. Synthesis and characterization of mesoporous silicon carbide. Microporous and Mesoporous Materials 60 (2003): 207-212.
- [44] Cheng, T.W., and Hsu, C.W. A study of silicon carbide synthesis from waste serpentine. Chemosphere 64 (2006): 510-514.

- [45] Rouquerol, F., Rouquerol, J., and Sing, K. Chapter 3 - Methodology of Adsorption at the Gas-Solid Interface. Adsorption by Powders and Porous Solids, 51-92. London: Academic Press, 1999.
- [46] Sing, K.S.W., et al. Reporting physisorption data for gas/solid systems with special reference to the determination of surface area and porosity (Recommendations 1984). Pure and Applied Chemistry 57 (1985): 603-619.

APPENDICES

APPENDIX A

CALCULATION OF MOLAR RATIO OF SILICA AND CARBON IN PRF GEL COMPOSITE

2.7 g of Resorcinol ($C_6H_4(OH)_2$)

↓
÷ 110 (M_w of $C_6H_4(OH)_2$)

0.025 mol of $C_6H_4(OH)_2$

↓
6 mol of C = 1 mol of $C_6H_4(OH)_2$

0.147 mol of C in Resorcinol

0.0106 g of Na_2CO_3

↓
÷ 106 (M_w of Na_2CO_3)

0.0001 mol of Na_2CO_3

↓
1 mol of C = 1 mol of Na_2CO_3

0.0001 mol of C in Na_2CO_3

0.692 g of Phenol ($C_6H_5(OH)$)

↓
÷ 94.11 (M_w of $C_6H_5(OH)$)

0.0074 mol of $C_6H_5(OH)$

↓
6 mol of C = 1 mol of $C_6H_5(OH)$

0.044 mol of C in Phenol

5.165 g of Formaldehyde (HCHO)

↓
÷ 30.03 (M_w of HCHO)

0.172 mol of HCHO

↓
1 mol of C = 1 mol of HCHO

0.172 mol of C in HCHO



6 mol of C = 1 mol of APTMS



1 mol of Si = 1 mol of APTMS

Molar ratio of carbon and silicon =

$$\frac{\text{Mole of Si in APTMS}}{\text{Mole of C in Resorcinol} + \text{Mole of C in Phenol} + \text{Mole of C in HCHO} + \text{Mole of C in Na}_2\text{CO}_3 + \text{Mole of C in APTMS}}$$

$$\text{Molar ratio of carbon and silicon} = \frac{\text{Mole of APTMS}}{0.147 + 0.044 + 0.172 + 0.0001 + 6(\text{Mole of APTMS})}$$

For example, Molar ratio of carbon and silicon = 0.03

$$\text{From calculation, } 0.05 = \frac{\text{Mole of APTMS}}{0.147 + 0.044 + 0.172 + 0.0001 + 6(\text{Mole of APTMS})}$$

$$\text{Get, Mole of APTMS} = 0.026$$

$$= 4.662 \text{ g of APTMS}$$

APPENDIX B

DATA OF SURFACE AREA AND AVG. PORE DIAMETER

Table B.1 Data of surface area and average pore diameter of pyrolyzed silica/PRF composites after being calcined at 400°C for 2 h.

Conditions (molar ratio)	Surface area (m ² /g)	Average pore diameter (nm)
P/R 0.3, SiO ₂ /C 0.03	5.714	3.72
P/R 0.3, SiO ₂ /C 0.05	3.536	3.72
P/R 0.3, SiO ₂ /C 0.07	4.584	3.29
P/R 0.5, SiO ₂ /C 0.05	45.63	3.29
P/R 1.0, SiO ₂ /C 0.05	31.61	3.72
P/R 1.5, SiO ₂ /C 0.05	25.39	3.29
Neat P, SiO ₂ /C 0.05	0.119	5.43
Neat R, SiO ₂ /C 0.05	293.1	2.41
P/R 0.3, SiO ₂ /C 0.03 (Sol)	328.0	21.5
P/R 0.3, SiO ₂ /C 0.05 (Sol)	175.1	13.9
P/R 0.3, SiO ₂ /C 0.07 (Sol)	87.19	21.5

Table B.2 Data of surface area and average pore diameter of pyrolyzed silica/PRF composites after being calcined at 450°C for 2 h.

Conditions (molar ratio)	Surface area (m²/g)	Average pore diameter (nm)
P/R 0.3, SiO ₂ /C 0.03	411.5	3.29
P/R 0.3, SiO ₂ /C 0.05	435.5	3.29
P/R 0.3, SiO ₂ /C 0.07	306.3	3.29
P/R 0.5, SiO ₂ /C 0.05	377.2	3.29
P/R 1.0, SiO ₂ /C 0.05	343.8	3.29
P/R 1.5, SiO ₂ /C 0.05	244.6	3.29
Neat P, SiO ₂ /C 0.05	9.980	5.43
Neat R, SiO ₂ /C 0.05	465.3	3.29
P/R 0.3, SiO ₂ /C 0.03 (Sol)	487.0	21.5
P/R 0.3, SiO ₂ /C 0.05 (Sol)	290.0	13.9
P/R 0.3, SiO ₂ /C 0.07 (Sol)	321.7	13.9

Table B.3 Data of surface area and average pore diameter of pyrolyzed silica/PRF composites after being calcined at 500°C for 2 h.

Conditions (molar ratio)	Surface area (m²/g)	Average pore diameter (nm)
P/R 0.3, SiO ₂ /C 0.03	453.3	3.29
P/R 0.3, SiO ₂ /C 0.05	435.5	3.29
P/R 0.3, SiO ₂ /C 0.07	542.8	3.29
P/R 0.5, SiO ₂ /C 0.05	530.4	3.29
P/R 1.0, SiO ₂ /C 0.05	536.7	3.29
P/R 1.5, SiO ₂ /C 0.05	517.3	3.29
Neat P, SiO ₂ /C 0.05	437.5	2.41
Neat R, SiO ₂ /C 0.05	459.6	3.29
P/R 0.3, SiO ₂ /C 0.03 (Sol)	459.5	13.9
P/R 0.3, SiO ₂ /C 0.05 (Sol)	253.9	13.9
P/R 0.3, SiO ₂ /C 0.07 (Sol)	n/a	n/a

Table B.4 Data of surface area and average pore diameter of silicon nitride product after final calcination at 800°C for 8 h. The pyrolyzed silica/PRF composites were calcined at 400°C for 2 h.

Conditions (molar ratio)	Surface area (m²/g)	Average pore diameter (nm)
P/R 0.3, SiO ₂ /C 0.03	189.6	4.78
P/R 0.3, SiO ₂ /C 0.05	248.3	5.43
P/R 0.3, SiO ₂ /C 0.07	55.20	5.43
P/R 0.5, SiO ₂ /C 0.05	271.9	5.43
P/R 1.0, SiO ₂ /C 0.05	134.0	7.05
P/R 1.5, SiO ₂ /C 0.05	138.1	4.78
Neat P, SiO ₂ /C 0.05	420.4	5.43
Neat R, SiO ₂ /C 0.05	285.3	4.78
P/R 0.3, SiO ₂ /C 0.03 (Sol)	60.90	13.9
P/R 0.3, SiO ₂ /C 0.05 (Sol)	88.57	3.29
P/R 0.3, SiO ₂ /C 0.07 (Sol)	29.49	16.1

Table B.5 Data of surface area and average pore diameter of silicon nitride product after final calcination at 800°C for 8 h. The pyrolyzed silica/PRF composites were calcined at 450°C for 2 h.

Conditions (molar ratio)	Surface area (m²/g)	Average pore diameter (nm)
P/R 0.3, SiO ₂ /C 0.03	173.1	4.21
P/R 0.3, SiO ₂ /C 0.05	223.6	3.29
P/R 0.3, SiO ₂ /C 0.07	60.00	9.21
P/R 0.5, SiO ₂ /C 0.05	75.47	10.5
P/R 1.0, SiO ₂ /C 0.05	101.8	4.78
P/R 1.5, SiO ₂ /C 0.05	97.49	5.43
Neat P, SiO ₂ /C 0.05	395.6	4.78
Neat R, SiO ₂ /C 0.05	261.0	4.78
P/R 0.3, SiO ₂ /C 0.03 (Sol)	40.69	13.9
P/R 0.3, SiO ₂ /C 0.05 (Sol)	77.19	3.29
P/R 0.3, SiO ₂ /C 0.07 (Sol)	78.00	13.9

Table B.6 Data of surface area and average pore diameter of silicon nitride product after final calcination at 800°C for 8 h. The pyrolyzed silica/PRF composites were calcined at 500°C for 2 h.

Conditions (molar ratio)	Surface area (m²/g)	Average pore diameter (nm)
P/R 0.3, SiO ₂ /C 0.03	53.22	3.29
P/R 0.3, SiO ₂ /C 0.05	76.60	3.72
P/R 0.3, SiO ₂ /C 0.07	51.90	3.72
P/R 0.5, SiO ₂ /C 0.05	99.70	3.29
P/R 1.0, SiO ₂ /C 0.05	82.00	3.29
P/R 1.5, SiO ₂ /C 0.05	140.4	3.29
Neat P, SiO ₂ /C 0.05	74.00	4.21
Neat R, SiO ₂ /C 0.05	146.8	3.29
P/R 0.3, SiO ₂ /C 0.03 (Sol)	39.40	13.9
P/R 0.3, SiO ₂ /C 0.05 (Sol)	45.99	3.29
P/R 0.3, SiO ₂ /C 0.07 (Sol)	46.20	3.72

APPENDIX C

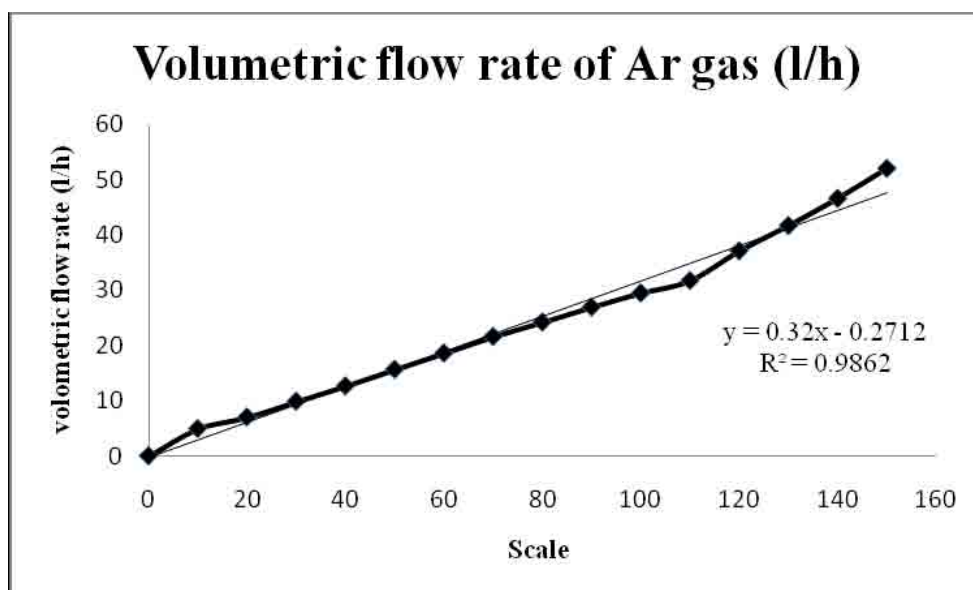
CALIBRATION CURVES FOR GAS FLOW METER
OF SYNTHESIS GAS

Figure C.1 The calibration curve of argon.

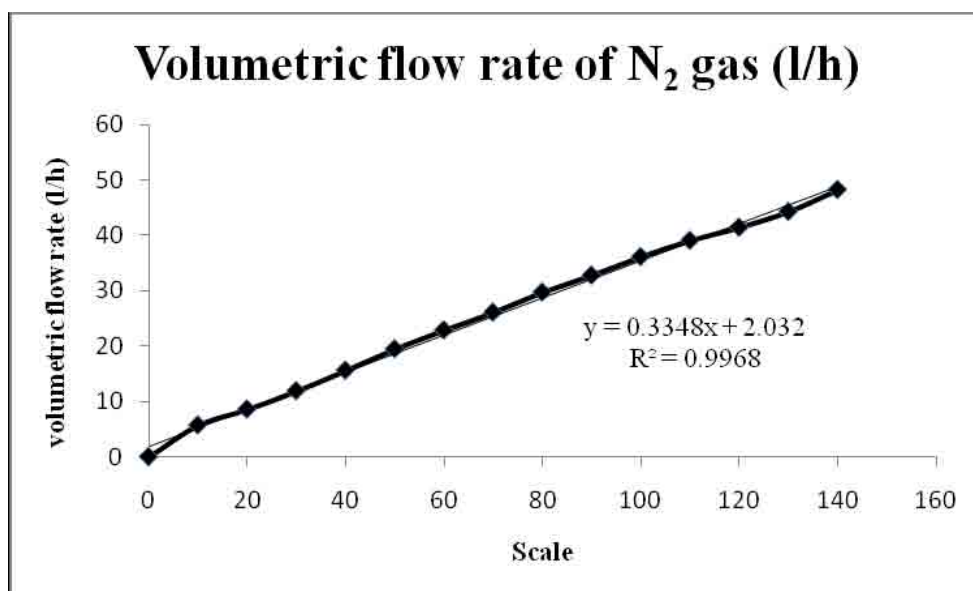


Figure C.2 The calibration curve of nitrogen.

APPENDIX D

CALCULATION OF THE CRYSTALLITE SIZE

Calculation of the crystallite size by Debye-Scherrer equation

The crystallite size was calculated from the width at half-height of the diffraction peak of XRD pattern using the Debye-Scherrer equation.

From Scherrer equation:

$$D = \frac{K\lambda}{\beta \cos \theta} \quad (\text{D.1})$$

- where
- D = Crystallite size, Å
 - K = Crystallite-shape factor = 0.9
 - λ = X-ray wavelength, 1.5418 Å for CuK α
 - θ = Observed peak angle, degree
 - β = X-ray diffraction broadening, radian

The X-ray diffraction broadening (β) is the pure width of a powder diffraction, free of all broadening due to the experimental equipment. Standard quartz is used to observe the instrumental broadening since its crystallite size is larger than 2000 Å. The X-ray diffraction broadening (β) can be obtained by using Warren's formula.

From Warren's formula:

$$\beta^2 = B_M^2 - B_S^2 \quad (\text{D.2})$$

$$\beta = \sqrt{B_M^2 - B_S^2}$$

Where B_M = The measured peak width in radians at half peak height.

B_S = The corresponding width of a standard material.

Example: Calculation of the crystallite size of silicon nitride

The half-height width of diffraction peak = 0.13°

$$= 0.00466 \text{ radian}$$

The corresponding half-height width of peak of quartz = 0.00225 radian

$$\begin{aligned} \text{The pure width} &= \sqrt{B_M^2 - B_S^2} \\ &= \sqrt{(0.00466)^2 - (0.00225)^2} \\ &= 0.00408 \text{ radian} \end{aligned}$$

$$\beta = 0.00408 \text{ radian}$$

$$2\theta = 30.91^\circ$$

$$\theta = 15.45591^\circ$$

$$\lambda = 1.5418 \text{ \AA}$$

$$\begin{aligned} \text{The crystallite size} &= \frac{0.9 \times 1.5418}{0.00408 \cos 15.455} = 352.6 \text{ \AA} \\ &= 35.26 \text{ nm} \end{aligned}$$

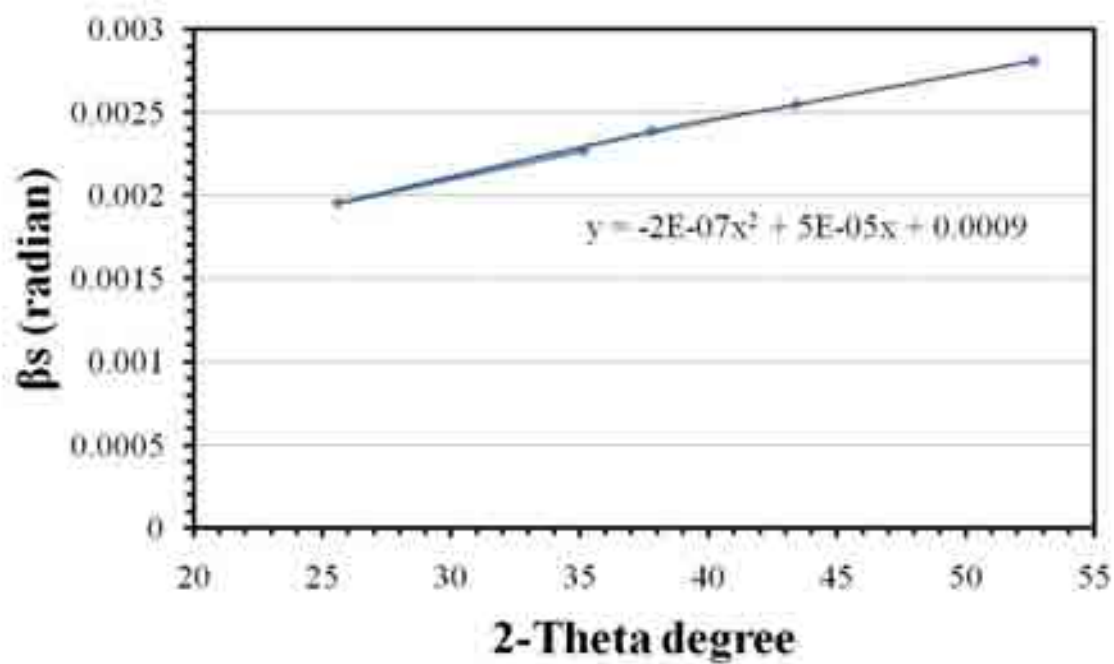


Figure D.1 The plot indicating the value of line broadening due to the equipment. The data were obtained by using quartz as standard.

APPENDIX E**LIST OF PUBLICATION**

1. Marisa Meechoonuck, Varong Pavarajarn, “synthesis of porous silicon nitride from silica/carbon composite derived from phenol-resorcinol-formaldehyde gel”, Pure and Applied Chemistry International Conference (PACCON2012), Chiang Mai, Thailand, January 11-13, 2012.

VITA

Miss. Marisa Meechoonuck was born on 11 February, 1988, in Bangkok, Thailand. She received the Bachelor's Degree of Engineering with a major in Chemical Engineering from Chulalongkorn University, *Bangkok* in April 2010. She continued her Master study in the major in Chemical Engineering at Chulalongkorn University, Bangkok, Thailand in May 2010.